From Channels to Cross Bridges

PROGRAM

July 13–16, 1991
Bar Harbor, Maine

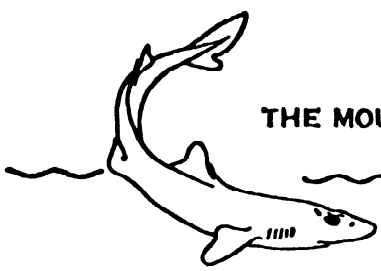

THE MOUNT DESERT ISLAND *Biological Laboratory*

AMERICAN PHYSIOLOGICAL SOCIETY

COUNCIL

Norman Staub	**Shu Chien**	**Stanley G. Schultz**
President	Past-President	President-Elect

Councillors

Helen J. Cooke	Brian R. Duling	L. Gabriel Navar
Allen W. Cowley	John E. Hall	David J. Ramsay

Ex Officio Members

Norman P. Alpert	Martin Frank	Leonard S. Jefferson
John S. Cooke	Carl V. Gisolfi	William S. Spielman

ORGANIZING COMMITTEE

Sir Andrew Huxley
Honorary Chairman

Lord Adrian	Makoto Endo	Lee Peachey
Knox Chandler	Yale Goldman	Martin Morad
Setsuro Ebashi		

ACKNOWLEDGEMENTS

The Society and Organizing Committee gratefully acknowledges the contributions received in support of this conference from:

Abbott Laboratories
Adams & List Associates, Ltd.
American Cyanamid Company
Axon Instruments, Inc.
Berlex Laboratories
Bristol Myers Squibb
Cardiac Muscle Society
Dagan Corporation
Eli Lilly Company
GIBCO BRL
Glaxo Inc. Research Institute
Merck Sharp & Dohme Research Laboratories
Miles, Inc./Bayer AG
Mount Desert Island Biological Laboratories
Philadelphia Physiological Society
Sutter Instrument Company
Uehara Memorial Foundation
Wyeth-Ayerst Research

DAILY SHUTTLE BUS SERVICE

Shuttle bus service will be available between the Regency Hotel and MDI High School Sunday, July 14 through Tuesday, July 16. Buses will leave promptly from the main entrance of each facility at the times listed below.

SUNDAY

7:30 AM – Hotel to High School
2:30 PM – High School to Hotel
6:30 PM – Hotel to High School
10:30 PM – High School to Hotel

MONDAY

7:30 AM – Hotel to High School
5:15 PM – High School to Hotel

TUESDAY

7:30 AM – Hotel to High School
4:45 PM – High School to Hotel

AIRPORT TRANSPORTATION

Bangor International Airport is located 50 miles west of Bar Harbor, approximately a one-hour drive. Taxi service is available from the airport to the island.

BUS SERVICE – BANGOR AIRPORT/BAR HARBOR

Limited bus service will be available on Saturday, July 13, from the Bangor Airport to the Bar Harbor Regency Hotel. One 15-passenger bus will be available at the times listed below on a first-come first-served basis. The buses will be located outside the Main Exit Doors, street level. Passengers will be required to show a registration badge to gain entry on the bus.

Saturday, July 13, 1991
From Bangor Airport to Bar Harbor Regency Hotel

9:00 AM	1:30 PM	6:00 PM
10:30 AM	3:00 PM	7:30 PM
12:00 Noon	4:30 PM	9:00 PM
		10:30 PM

This bus service will also be available for a return trip on Wednesday, July 17, to Bangor Airport from the Bar Harbor Regency Hotel at the times listed below.

Wednesday, July 17, 1991
From Bar Harbor Regency Hotel to Bangor Airport

6:00 AM	9:00 AM	12:00 Noon
7:00 AM	10:00 AM	1:00 PM
8:00 AM	11:00 AM	3:00 PM
		4:00 PM

ON-SITE REGISTRATION

The registration fee includes the Opening Receptor, Lobster/Clam Bake, entrance to the symposia and poster sessions, and receipt of the Program/Abstract Volume.

Locations:

Bar Harbor Regency Hotel: Registration Counter
MDI High School: Library

Hours:

Saturday, July 13, Regency Hotel.....7:30 AM–9:00 PM
Sunday, July 14, MDI High School ....8:00 AM–2:30 PM
Regency Hotel .....3:30 PM–4:30 PM
Monday, July 15, MDI High School ...8:00 AM–4:30 PM

PROGRAM/ABSTRACT VOLUME

The August 1991 issue of *The Physiologist* contains the contributed abstracts and program for the meeting. Registrants may pick-up issues during the registration hours listed above.

CONTINUING MEDICAL EDUCATION CREDIT

The Conference has been certified for CME Category 1 credit on an hour-for-hour basis. CME forms, which must be completed and returned to receive credit, will be available at the registration areas.

OPENING RECEPTION

An Opening Reception will be held at the Mount Desert Island Biological Laboratory Co-Op on Saturday, July 13, from 5:00-9:00 PM. Shuttle buses will run between the hotel and laboratory on an hourly basis starting at the hotel at 4:30 PM with the last bus leaving the lab at 9:30 PM.

LOBSTER/CLAM BAKE

All registrants are invited to attend the Lobster and Clam Bake from 7:00-10:00 PM on Monday, July 15. A dinner ticket will be required for admittance. **Each registrant must pick-up a dinner ticket by 9:00 AM Sunday, July 14.** Non-registered guests and family members may purchase tickets on a first-come first-served basis. Tickets will be available for pick-up and/or purchase on Saturday, July 13 at the Regency Hotel, Registration Counter, from 7:30 AM-9:00 PM and on Sunday, July 14 at the MDI High School Library from 8:00-9:00 AM.

BOX LUNCHES

Box lunches will be provided to registrants on Monday, July 15 and Tuesday, July 16 from 12:30-2:30 PM in the MDI High School Cafeteria.

APS CONFERENCE

FROM CHANNELS TO CROSS BRIDGES

DAILY SCHEDULE

SUNDAY

Shuttle Bus Schedule

7:30 AM – To High School
2:30 PM – To Hotel
6:30 PM – To High School
10:30 PM – To Hotel

Opening Greetings
Sunday, 8:30-8:45 AM

8:30 Welcome from APS. **Stanley G. Schultz,** President-Elect.
8:35 Welcome from MDIBL. **Frank Epstein,** President.
8:40 Welcome from Organizing Committee. **Martin Morad,** Chair.

Plenary Lecture
Sunday, 8:45-9:30 AM

1.0 Molecular Insights into Ionic Channels

Speaker: **Shosaku Numa.** Kyoto Univ., Japan

Morning Symposium
Sunday, 9:30 AM-12:30 PM

2.0 Molecular Understanding into Ionic Channels

Chaired: **Richard Tsien,** Stanford Univ.
Wolfgang Trautwein, Univ. of Saarlandes, Homburg, Germany

9:30 Introduction.
9:40 Molecular Properties of Voltage Gated Na^+ Channels.
William Catterall. Univ. of Washington.
10:00 Discussion.
10:10 Gating Currents of Na^+ and K^+ Channels: Implications for H&H Model.
Walter Stühmer. Max-Planck-Inst., Gottingen, Germany.
10:30 Discussion.
10:40 Break.
11:00 Regulation of Ca^{2+} Channels by its Subunits.
Franz Hofmann. Univ. Munich, Germany.
11:20 Discussion.
11:30 Permeation through the Ca^{2+} Channel.
Hans Dieter Lux. Max-Planck-Inst., Munich, Germany.
11:50 Discussion.
12:00 Molecular Studies on Ca^{2+} Channels.
Arnold Schwartz. Univ. of Cincinnati.
12:10 Discussion.
12:15 Receptor-Mediated Regulation of Ca^{2+} Channel.
M. Hosey. Northwestern Univ.
12:25 Discussion.

Posters
Sunday, 12:30-2:30 PM

3.0 Ion Channel Regulation

Board #

A-1 **3.1** A comparison of dihydropyridine receptor and functional L-type Ca channel densities in heart. **T.L. Creazzo, S. Aiba, S. Redmond, and L. Hancock.** Med. Col. Georgia.
A-2 **3.2** Abnormality in the ryanodine receptor calcium release channel in human malignant hyperthermia. **T.E. Nelson.** Univ. of Texas Hlth. Sci. Ctr., Houston.
A-3 **3.3** Discontinuous volume transitions in the ectoplasm and the process of action potential production. **I. Tasaki.** Natl. Inst. Mental Hlth.
A-4 **3.4** Sulfhydryl-specific reagents activate a calcium current and enhance mechanical responses in an invertebrate striated muscle. **C. Zuazaga, L. Lizardi, M.C. Garcia, and J.A. Sanchez.** Univ. of Puerto Rico.
A-5 **3.5** Characterization of the Ca^{2+} entry channel in the basolateral plasma membrane of rat parotid gland acinar cells. **T. Lockwich, B.J. Baum, and I.S. Ambudkar.** NIH.
A-6 **3.6** Na^+ permeability change predicted proportional to gating current. **D.M. Easton.** Florida State Univ.
A-7 **3.7** Constant fields and constant gradients in open ionic channels. **R.S. Eisenberg, D.P. Chen, and V. Barcilon.** Rush Med. Col.
A-8 **3.8** Does phosphorylation increase the open probability of calcium channel of cardiac muscle? **R. Ochi, T. Nakamura, and H-Y. Li.** Juntendo Univ., Tokyo, Japan.
A-9 **3.9** Modelling of cardiac sodium channel and the relationship between V_{max} and I_{Na} under physiological conditions. **J. Toyama, T. Anno, A. Taniguchi, M. Shirakawa, and S. Usi.** Toyohashi Univ. of Tech., Japan.
A-10 **3.10** Na^+ channel isotypes in adult rat dorsal root ganglion neurons identified by electrophysiological and molecular biological techniques. **J.M. Caffrey, L.D. Brown, J.G.R. Emanuel, D.L. Eng, S.G. Waxman, and J.D. Kocsis.** Yale Univ. and VA Med. Ctr., West Haven, CT.
A-11 **3.11** Ion channel properties are altered by lipid bilayer composition. **H.M. Chang, S.M. Gruner, and R. Gruener.** Univ. of Arizona and Princeton Univ.
A-12 **3.12** Regulation of apical epithelial Na^+ channels by actin filament organization. **A.G. Prat, D.A.**

Ausiello, and H.F. Cantiello. Mass. General Hosp. and Harvard Med. Sch.

A-13 **3.13** Ion regulation by a cytoskeletal-electrodynamic network. **H.F. Cantiello and D.S. Kim.** Mass. General Hosp. and Harvard Med. Sch.

A-14 **3.14** Purification of cardiac myocyte cultures for use in calcium channel expression studies. **A. Lokuta, W.J. Lederer, and T.B. Rogers.** Univ. of Maryland, Baltimore.

A-15 **3.15** Single-channel kinetics of NMDA receptors in Xenopus spinal neurons. **Y. Zhang and A. Auerbach.** SUNY, Buffalo.

A-16 **3.16** Properties of endogenous voltage-dependent Na channels in Xenopus oocytes. **D.S. Krafte and W.A. Volberg.** Sterling Res. Group, Rensselaer, NY.

A-17 **3.17** Frequency-dependent effects of sea anemone toxins on refractoriness and action potential duration: lack of correlation with effects at cardiac sodium channels. **G.M. Briggs, D. Krafte, P. Canniff, W. Volberg, and A. Ezrin.** Sterling Res. Group, Rensselaer, NY.

A-18 **3.18** Calcium channel modulation by norepinephrine and GABA. **H. Cox and K. Dunlap.** Tufts Med. Sch.

A-19 **3.19** Tension sensitivity of alamethicin channel conductance state distribution and kinetics. **L.R. Opsahl and W.W. Webb.** Cornell Univ.

A-20 **3.20** Mutational effects and functional role of ionic currents in "giant" Drosophila neurons. **M. Saito and C.-F. Wu.** Univ. of Iowa.

A-21 **3.21** Ras induction of sodium channels in medullary thyroid carcinoma cells. **S.A. DeRiemer, B.D. Nelkin, and H. Tamir.** Johns Hopkins Med. Inst.

A-22 **3.22** Stretch activation of the S channel in mechanosensory neurons of Aplysia. **D.H. Vandorpe and C.E. Morris.** Loeb Inst., Ottawa Civic Hosp., Canada.

A-23 **3.23** Characterization of ATP-regulated K^+ channels in human airway epithelia. **J.G. Fitz, J.R. Yankaskas, and M.J. Stutts.** Duke Univ. and Univ. of North Carolina.

A-24 **3.24** Regulation of chloride channels in human skeletal muscle. **C. Fahlke, E. Zachar, and R. Rudel.** Univ. of Ulm, Germany.

A-25 **3.25** Voltage-sensitive and solvent-sensitive processes in ion channel gating: effects of osmotic stress on crayfish sodium channels. **M.D. Rayner and J.G. Starkus.** Univ. of Hawaii.

A-26 **3.26** Calcium-sensitive chloride currents in vascular smooth muscle cells. **C.R. White, T.A. Brock, and R.L. Shoemaker.** Univ. of Alabama.

A-27 **3.27** Unitary but not macroscopic conductance of human connexin43 gap junction channels is altered by phosphorylating treatments. **A.P. Moreno, G.I. Fishman, and D.C. Spray.** Albert Einstein Col. Med.

A-28 **3.28** Regulation of L-type Ca^{2+}-channels in skeletal muscle by cAMP-dependent protein kinase. **A. Sculptoreanu, T. Scheuer, and W.A. Catterall.** Univ. of Washington and Univ. of Sherbrooke, Canada.

A-29 **3.29** Acetylcholine activates a chloride conductance in mammalian tracheal myocytes. **L.J. Janssen and S.M. Sims.** Univ. of Western Ontario, Canada.

A-30 **3.30** Supersensitivity to tetrodotoxin and lidocaine of sea anemone toxin II-modified Na channels in guinea pig ventricular muscle. **M. Nishio, T. Ohmura, S. Kigoshi, and I. Muramatsu.** Fukui Med. Sch., Japan.

A-31 **3.31** Simulation of the role of water in ion channel gating. **M.E. Green.** City Col. of CUNY, New York.

A-32 **3.32** A Ca^{2+} channel with small conductance and BAY-K-8644 sensitivity in capillary endothelial cells. **A. Feltz, J.-L. Bossu, A. Elhamdani, and F. Tanzi.** CNRS, Strasbourg, France.

A-33 **3.33** Ca^{2+}-dependent facilitation and inhibition of the $GABA_A$ response in cultured porcine melanotrophs. **D. Mouginot, P. Feltz, and R. Schlicter.** CNRS, Strasbourg, France.

A-34 **3.34** On ion selection in Ca channels. **H.D. Lux.** Max-Planck-Inst., Martinsried, Germany.

A-35 **3.35** The synergism of calcium- and chloride-channels in characeae. **P.R. Andjus, D. Vučelić, A.A. Kateav, A.A. Alexandrov, and G.N. Berestovsky.** Inst. Gen. Physiol. Chem., Belgrade, Yugoslavia and Inst. Cell Biophysics, Moscow, USSR.

Evening Symposium
Sunday, 7:30-10:30 PM

4.0 New Approaches to Channel Function

Chaired: **Lord Adrian,** Pembroke Col., Cambridge, UK
Clay Armstrong, Univ. of Pennsylvania

7:30 **Introduction.**

7:40 Mechanisms of K^+ Channel Gating.
Richard Aldrich. Stanford Univ.

8:00 Discussion.

8:10 K^+ Channels and Their Regulation.
Arthur Brown. Baylor Col. Med.

8:30 Discussion.

8:40 Molecular Dentistry: Probing a K^+ Channel's Mouth.
Chris Miller. Brandeis Univ.

9:00 Discussion.

9:10 Break.

9:30 How to Build an Excitable Cell.
Henry Lester. California Inst. of Technol.

9:50 Discussion.

10:00 Molecular Genetic Dissection of Ca^{2+} Channel Function.
T. Tanabe. Kyoto Univ., Japan.

10:10 Discussion.

10:15 Modulation of G Protein-Gated K^+ Channels by Arachadonic Acid.
Yoshihisa Kurachi. Mayo Clin.

10:25 Discussion.

MONDAY

Shuttle Bus Schedule

7:30 AM – To High School
5:15 PM – To Hotel

Morning Symposium
Monday, 8:30 AM-12:00 Noon

5.0 Excitation-Contraction Coupling: Signalling

Chaired: **Knox Chandler,** Yale Univ.
Makoto Endo, Tokyo Univ., Japan

8:30 Introduction.
8:40 Comparative Molecular Architecture of E-C Coupling.
Clara Franzini-Armstrong. Univ. of Pennsylvania.
9:00 Discussion.
9:10 The Structure of SR Ca^{2+} Release Channel and its Regulation by Ca^{2+}.
Gerhard Meissner. Univ. of North Carolina.
9:30 Discussion.
9:40 Regulation of Ca^{2+} Release and Uptake in Cardiac Myocytes.
Martin Morad. Univ. of Pennsylvania.
10:00 Discussion.
10:10 Break.
10:30 Molecular Biology of DHP Receptor and Charge Movement.
Kurt Beam. Colorado State Univ.
10:50 Discussion.
11:00 Function and Mode of Action of Small G Proteins.
Yoshimi Takai. Kobe Univ., Japan.
11:20 Discussion.
11:30 Charge Movement Associated with Voltage Sensors of Cardiac and Skeletal Muscle.
Eduardo Rios. Rush Med. Col.
11:40 Discussion.
11:45 Signal Transduction in Smooth Muscle.
Avril Somlyo. Univ. of Virginia.
11:55 Discussion.

Posters
Monday, 12:00 Noon-2:00 PM

6.0 Ion Channel Structure

Board #

A-1 **6.1** Regulation of the cardiac a1 calcium channel subunit by skeletal muscle B and Y subunits. **X. Wei, E. Perez-Reyes, A. Lacerda, L. Birnbaumer, and A.M. Brown.** Baylor Col. of Med.

A-2 **6.2** Possible brain channels: a comparison of penetration and retention of the p-I-131-iodobenzyl-amino derivatives of adamantane and isoborane. **M.K. Karimeddini, E.E. Leutzinger, H.K. Patel, and R.P. Spencer.** Univ. of Connecticut Hlth. Ctr.

A-3 **6.3** The gating mechanism of K channels as revealed by pore structure. **C-Y. Lee.** Advantage Capital Corp., Guilderland, NY.

A-4 **6.4** Ion selectivity profiles of amphotericin B channels in lipid vesicles. **S.C. Hartsel, S.K. Benz, W. Ayenew, and T. Stephan.** Univ. of Wisconsin, Eau Claire.

A-5 **6.5** A novel physical model for voltage-dependent gating of L-type calcium channels. **C.A. Doupnik and R.Y.K. Pun.** Univ. of Cincinnati.

A-6 **6.6** Calcium permeation of voltage-dependent sodium channels at large driving forces. **B.B. Hogans and B.K. Krueger.** Univ. of Maryland, Baltimore.

A-7 **6.7** A reexamination of the mechanism of blockade of the delayed rectifier by tetraethylammonium ions: must the channel open for blockade to occur? **J.R. Clay.** NIH.

A-8 **6.8** A detailed structural model of the transmembrane portion of voltage-gated potassium channels. **H.R. Guy and S.R. Durell.** NCI, NIH.

A-9 **6.9** Expressed Na channel clones differ in their sensitivity to external [Ca]. **M. Chahine, L. Chen, R. Kallen, R. Barchi, and R. Horn.** Roche Inst. of Molec. Biol. and Univ. of Pennsylvania.

A-10 **6.10** Characterization of calcium entry and a novel calcium channel cloned from murine erythroleukemia cells. **B. Gillo, Y-S. Ma, Q. Liu, D-M. Yang, and A.R. Marks.** Mt. Sinai Sch. of Med., New York.

A-11 **6.11** A β-barrel model for the pore of the voltage-gated potassium channel. **S. Bogusz, A. Boxer, J.A. Drewe, G.E. Kirsch, H. Hartmann, M. Taglialatela, A.M. Brown, R. Joho, and D. Busath.** Brown Univ. and Baylor Col. of Med.

A-12 **6.12** Mutations in the leucine heptad repeat of shaker 29-4 alter the channel's activation without altering gating currents. **N.E. Schoppa, K. McCormack, M.A. Tanouye, and F.J. Sigworth.**

A-13 **6.13** Isolation and biochemical characterization of the rabbit brain ω-conotoxin GVIA receptor. **J. Sakamoto and K. P. Campbell.** Howard Hughes Med. Inst. and Univ. of Iowa.

Posters
Monday, 12:00 Noon-2:00 PM

7.0 Receptor-Effector Signalling and E-C Coupling

Board #

A-14 **7.1** Avian extended JSR: a challenge to direct contact signal transduction for coupling excitation to calcium-release in cardiac muscle. **J.R. Sommer, E. Bossan, and R. Nassar.** Duke Univ. Med. Ctr. and VA Hosp., Durham.

A-15 **7.2** Role of paravalbumin in frog skeletal muscle

relaxation. **J.A. Rall, T.-T. Hou, and J.D. Johnson.** Ohio State Univ.

A-16 **7.3** Inhibitory mechanisms of K channel openers on agonist-induced contractions in coronary artery. **T. Yanagisawa and N. Taira.** Tohoku Univ., Sendai, Japan.

A-17 **7.4** Regulation of contractile properties by muscarinic receptor stimulation in ferret ventricular muscle. **S. Kurihara, K. Hongo, and E. Tanaka.** The Jikei Univ., Tokyo, Japan.

A-18 **7.5** The Ca^{2+}-sensitivity of the photoprotein halistaurin is not influenced by physiological concentrations of Mg^{2+}. **J.R. Blinks and D.D. Caplow.** Univ. of Washington.

A-19 **7.6** Interactions of the α subunits of the skeletal muscle dihydropyridine receptor. **B.E. Flucher, J.L. Phillips, and J.A. Powell.** NIH and Smith Col., Northampton, MA.

A-20 **7.7** Phosphoinositide hydrolysis and positive inotropic effect induced by endothelin in the rabbit ventricular muscle. **M. Endoh and M. Takanashi.** Yamagata Univ., Japan.

A-21 **7.8** Selective inhibition by staurosporine and phorbol ester of the positive inotropic effect mediated by α-1 adrenergic receptors. **M. Endoh, M. Takanashi, and I. Norota.** Yamagata Univ., Japan.

A-22 **7.9** Cholesterol modulates the membrane binding of 1,4-dihydropyridine Ca^{2+} channel blockers. **R.P. Mason and L. Shajenko.** Univ. of Connecticut Hlth. Ctr.

A-23 **7.10** Calcium-induced calcium release in crayfish muscle fibers. **S. Gyorke and P. Palade.** Univ. of Texas Med. Branch.

A-24 **7.11** ^{125}I-calmodulin binding to proteins in sarcolemmal membrane fractions from mammalian heart. **D.D. Doyle and Y. Guo.** Univ. of Chicago.

A-25 **7.12** Smooth muscle $[Ca^{2+}]_c$ in response to Ca^{2+} influx through voltage and receptor operated channels. **G. Isenberg, P. Schneider, and V.Y. Ganitkevich.** Univ. of Cologne, Germany.

A-26 **7.13** Intracellular sodium gradients in stimulated guinea pig ventricular myocytes: an x-ray microprobe study. **M.F. Wendt-Gallitelli and G. Isenberg.** Univ. of Tübingen and Univ. of Cologne, Germany.

A-27 **7.14** Development of peripheral couplings and triads reflects increase in dihydropyridine binding in chicken hind limb muscles. **H. Takekura and C. Franzini-Armstrong.** Univ. of Pennsylvania.

A-28 **7.15** Na/Ca exchange studies in frog phasic muscle cells. **H. Gonzalez-Serratos, E. Castillo, M. Rozycka, and H. Rasgado-Flores.** Univ. of Maryland, Baltimore and The Chicago Med. Sch.

A-29 **7.16** Characterization of a frog skeletal muscle contraction modulator. **N.M. Kumbaraci.** Stevens Inst. of Tech., Hoboken, NJ.

A-30 **7.17** Dihydropyridine receptors are primarily functional L-type Ca channels, but are outnumbered by ryanodine receptors in rabbit cardiac myocytes. **D.M. Bers, W.Y.W. Lew, L.V. Hryshko, and V.M. Stiffel.** Univ. of California, Riverside and UCSD.

A-31 **7.18** A membrane model for cytosolic calcium oscillations: a study using Xenopus oocytes. **M.S. Jafri, P. Pasik, S. Vajda, and B. Gillo.** Mt. Sinai Sch. of Med., New York.

Posters
Monday, 12:00 Noon-2:00 PM

8.0 Cardiac Electrophysiology

Board #

A-32 **8.1** Drug-induced after-depolarizations and triggered activity occur in a select subpopulation of cells (M cells) in the deep subepicardium of the canine ventricle. **S. Sicouri and C. Antzelevitch.** Masonic Med. Res. Lab., Utica, NY.

A-33 **8.2** Pinacidil-induced reentrant arrhythmias in isolated canine ventricular epicardium. **J.M. Di Diego and C. Antzelevitch.** Masonic Med. Res. Lab., Utica, NY.

Afternoon Symposium
Monday, 2:00-5:15 PM

9.0 Mechanisms of Muscle Contraction

Chaired: **Yale Goldman,** Univ. of Pennsylvania
Setsuro Ebashi, Natl. Inst. Physiol. Sci., Aichi, Japan

2:00 **Introduction.**

2:10 The Active Site of Myosin: Implications for Contractile Mechanisms.
Ralph Yount. Washington State Univ.

2:30 Discussion.

2:40 Sub-Piconewton-Level Force Fluctuations in Actomyosin *in vitro.*
Toshio Yanagida. Osaka Univ., Japan.

3:00 Discussion.

3:10 Spectroscopic Probes of Muscle Fibers.
David Thomas. Univ. of Minnesota.

3:30 Discussion.

3:40 Break.

4:00 Structure and Function of Actin-Myosin Systems.
Takeyukii Wakabayashi. Univ. of Tokyo, Japan.

4:20 Discussion.

4:30 The Orientation of the Neck Region of the Myosin Head Measured by Spin Probes.
Roger Cooke. UCSF.

4:40 Discussion.

4:45 Step Size for Cross Bridge Interactions in Intact Muscle Fibers.
Vincenzo Lombardi. Univ. of Florence, Italy.

4:55 Discussion.

5:00 The Actomyosin ATPase in Muscle.
David R. Trentham. Natl. Inst. for Med. Res., London, UK.

5:10 Discussion.

TUESDAY

Shuttle Bus Schedule

7:30 AM – To High School
4:45 PM – To Hotel

Morning Symposium
Tuesday, 8:30 AM-12:00 Noon

10.0 Non-Muscle Motility

Chaired: **Mike Sheetz,** Washington Univ.
Fumio Oosawa, Aichi Inst. of Technol., Toyota, Japan

8:30 Introduction.
8:40 Manifestations of the Myosin Molecular Motor: Amoebae to Muscle.
James Spudich. Stanford Univ.
9:00 Discussion.
9:10 Bacterial Rotary Motors.
Howard Berg. Harvard Univ.
9:30 Discussion.
9:40 Chromosome/Spindle Motility.
Sharyn Endow. Duke Univ.
10:00 Discussion.
10:10 Break.
10:30 Biophysics of Kinesin- and Dysin-Based Motility.
Ron Vale. UCSF.
10:50 Discussion.
11:00 Mechanism of Kinesin and Cytoplasmic Dynein Movement.
Mike Sheetz. Duke Univ.
11:20 Discussion.
11:30 Imaging Bacterial Flagella.
Steven Block. Rowland Inst. of Sci., Cambridge, MA.
11:40 Discussion.
11:45 Mechanochemical Coupling in the Bacterial Flagellar Motor.
Shahid Khan. Albert Einstein Col. of Med.
11:55 Discussion.

Posters
Tuesday, 12:00 Noon-2:00 PM

11.0 Mechanisms of Muscle Contraction

Board #

A-1 **11.1** Muscle contraction mechanism theory: a simple engineering analysis of myoplasmic surface tension. **A.F. Metherell.** MRI Centers, Santa Ana, CA.

A-2 **11.2** Myosin light chain phosphorylation cooperatively activates crossbridge cycling in smooth muscle. **M.J. Siegman, T. Vyas, S. Mooers, S. Narayan, and T.M. Butler.** Jefferson Med. Col.

A-3 **11.3** Sub-piconewton-level force fluctuation of actomyosin in vitro. **T. Yanagida.** Osaka Univ., Japan.

A-4 **11.4** Spontaneous activation of smooth muscle late in isotonic relaxation. **N.L. Stephens, A. Halayko, K. Rao, X. Liu, and H. Jiang.** Univ. of Manitoba, Canada.

A-5 **11.5** Stochastic simulations of in vitro motility. **J.B. Patlak and D.M. Warshaw.** Univ. of Vermont.

A-6 **11.6** Thermodynamic studies on cardiac isomyosins. **G. Kaldor and D.R. Hoak.** VA Med. Ctr., Allen Park, MI and Wayne State Univ.

A-7 **11.7** Differential fluorescent labeling of the myosin ATPase. **T. Hiratsuka.** Asahikawa Med. Col., Hokkaido, Japan.

A-8 **11.8** Fluorescence studies within the regulatory light chain of skeletal myosin. **B.D. Hambly, W. Boey, E. Moisidis, and C.G. dos Remedios.** Sydney Univ., Australia.

A-9 **11.9** Time resolved x-ray diffraction measurement in single intact muscle fibres. **Y. Maéda, C.C. Ashley, M.A. Bagni, G. Cecchi, and P.J. Griffiths.** EMBL at DESY, Hamburg, Germany.

A-10 **11.10** Chemically skinned guinea pig taenia coli: the binding and possible role of creatine kinase. **J.F. Clark, P. Mateo, Z. Khuchua, and R. Ventura-Clapier.** INSERM, Univ. Paris-Sud, Orsay, France.

A-11 **11.11** Spontaneous oscillatory contraction of sarcomeres in myofibrils: synergistic effects of ADP and inorganic phosphate. **S. Ishiwata, T. Anazawa, T. Fujita, N. Fukuda, and K. Yasuda.** Waseda Univ., Tokyo, Japan.

A-12 **11.12** Kinetic studies of the state change of the muscle thin filament. **Y. Ishii and S.S. Lehrer.** Biomed. Res. Inst., Boston, MA.

A-13 **11.13** The effect of actin-myosin lattice spacing on force generation in skeletal muscle. **Y. Zhao and M. Kawai.** Univ. of Iowa.

A-14 **11.14** A simple stochastic model for motor proteins. **S. Leibler and D.A. Huse.** Ctr. d'Etudes de Saclay, France and Bell Labs., Murray Hill, NJ.

A-15 **11.15** Increased cross-bridges and force increase the calcium affinity of troponin in barnacle muscle fibers. **A.M. Gordon and E.B. Ridgway.** Univ. of Washington and Med. Col. Virginia.

A-16 **11.16** Comparison of the mechanical and electrophysiological effects of two isoquinoline alkaloids on rat cardiac tissue. **M.J. Su, P.J. Liu, Y.C. Nieh, and J.H. Lee.** Natl. Taiwan Univ. and Natl. Inst. of Chinese Med., Taipei, Taiwan.

A-17 **11.17** Vanadate and phosphate probe the energetics of cross bridge states during the force producing stroke in skeletal muscle. **G. Wilson, S. Shull, E. Pate, and R. Cooke.** UCSF.

A-18 **11.18** Stiffness changes associated with exercise-induced muscle injury in humans. **J.N. Howell, R. Conatser, G. Chleboun, and J. Cummings.** Ohio Univ. Col. Osteo. Med.

A-19 **11.19** Muscle fatigue in the frog semitendinosus:

the role of intracellular pH. **L.V. Thompson, E.M. Balog, and R.H. Fitts.** Marquette Univ.

A-20 **11.20** Maximal shortening velocity and ATPase activity of single slow- and fast-twitch rat muscle fibers. **J.M. Schluter, K.M. McDonald, and R.H. Fitts.** Marquette Univ.

A-21 **11.21** ATP hydrolysis and myofibril shortening. **E.W. Taylor.** Univ. of Chicago.

A-22 **11.22** Potassium channel inhibitors cause endothelium independent pulmonary arterial vasoconstriction. **S.L. Archer, J.M. Post, J.R. Hume, D.P. Nelson, and E.K. Weir.** Minneapolis VA Med. Ctr. and Univ. of Nevada, Reno.

A-23 **11.23** Kinetics of cross bridge cycling in the presence of MgADP in alpha-toxin permeabilized smooth muscle cells. **E. Nishiye, A.V. Somlyo, K. Török, and A.P. Somlyo.** Univ. of Virginia and Natl. Inst. for Med. Res., London, UK.

A-24 **11.24** Rate of regeneration of 12 nm power-stroke after sudden shortening of tetanized fiber from frog muscle. **G. Piazzesi, M. Linari, and V. Lombardi.** Univ. of Florence, Italy.

A-25 **11.25** Effects of aluminofluoride on skinned muscle fiber stiffness. **P.B. Chase, D.A. Martyn, M.J. Kushmerick, and A.M. Gordon.** Univ. of Washington.

A-26 **11.26** Computer simulations of mechanical transients in skeletal muscle fibers. **H. Shuman, J.A. Dantzig, and Y.E. Goldman.** Univ. of Pennsylvania.

A-27 **11.27** At low temperature and ionic strength AM-T --> AM-D-P is the rate limiting step of skeletal actomyosin-S1 ATP hydrolysis. **B. Belknap, X-Q. Wang, X-Z. Zhang, and H.D. White.** Eastern Virginia Med. Sch.

A-28 **11.28** Electron cryo-microscopy of actomyosin-S1 during steady state ATP hydrolysis. **J. Trinick and H. White.** Bristol Univ., UK and Eastern Virginia Med. Sch.

Posters
Tuesday, 12:00 Noon-2:00 PM

12.0 Non-Muscle Motility

Board #

A-29 **12.1** Effects of membrane depolarization on neurite outgrowth and microtubule polymerization equilibria in axons and dendrites of sympathetic neurons in culture. **C.H. Keith.** Univ. of Georgia.

A-30 **12.2** Kinesin unfolds at high ionic strength. **D.D. Hackney and J.D. Levitt.** Carnegie Mellon Univ.

A-31 **12.3** Measuring the isometric tension of kinesin molecules using the laser optical trap. **M.P. Sheetz and S.C. Kuo.** Duke Univ. Med. Ctr.

Posters
Tuesday, 12:00 Noon-2:00 PM

13.0 Novel Microscopic Techniques

Board #

A-32 **13.1** An electronic imaging system modified for microscopic studies of rapid events in live skeletal muscle cells. **S.R. Taylor, I.R. Neering, L.A. Quesenberry, and V.A. Morris.** Mayo Fndn.

A-33 **13.2** High speed video microscopy: myocyte striation pattern dynamics imaged at a 240 Hz field rate. **K.P. Roos.** UCLA.

A-34 **13.3** Evanescent wave microscopy: a simple optical configuration for motility studies. **J.M. Murray.** Univ. of Pennsylvania.

A-35 **13.4** Vasopressin-induced depolymerization of F-actin determined by confocal microscopy. **R.M. Hays, N. Franki, K. Holmgren, and K.E. Magnusson.** Albert Einstein Col. of Med. and Univ. of Linköping, Sweden.

Afternoon Symposium
Tuesday, 2:00-4:45 PM

14.0 Novel Microscopic Techniques

Chaired: **Lee Peachey,** Univ. of Pennsylvania
Keith Porter, Univ. of Pennsylvania

2:00 Introduction.

2:10 Structural Approaches to E-C Coupling: Confocal Microscopy of T-Systems.
Andrew Somlyo. Univ. of Virginia.

2:30 Discussion.

2:40 New Laser Microscopies.
Watt Webb. Cornell Univ.

3:00 Discussion.

3:10 Video Microscopy of Individual Microtubule Assembly Dynamics and Motility.
Edward Salmon. Univ. of North Carolina.

3:30 Discussion.

3:40 Atomic Force Microscopy of Biological Surfaces.
Helen Hansma. Univ. of California, Santa Barbara.

4:00 Discussion.

4:10 Closing Remarks.
Sir Andrew Huxley. Trinity Col., Cambridge, UK.

4:30 Final comments.
Martin Morad. Univ. of Pennsylvania.

From Channels to Cross Bridges

Sessions with Associated Abstracts

3.1

A COMPARISON OF DIHYDROPYRIDINE RECEPTOR AND FUNCTIONAL L-TYPE CA CHANNEL DENSITIES IN HEART. Tony L. Creazzo, Sumi Aiba, Shannon Redmond and Lesley Hancock. (Spon. Robert Godt). Department of Anatomy, Medical College of Georgia, Augusta, Georgia 30912.

We compared the densities of dihydropyridine (DHP) receptors and functional L-type Ca channels in ventricular myocytes from the day 11 embryonic chick ventricle. DHP receptors were quantified by Scatchard analysis using the DHP antagonist, [3H]-PN200-110. Ventricles contained an average of 259±11 fmol DHP receptors (n=3 determinations of 10-20 pooled ventricles each; ±SEM). The mean number of myocytes per ventricle was $14.4 \pm 4.2 \times 10^6$, as determined morphometrically. These data indicated an average of 10,830 sites/myocyte or 16.2 DHP receptors/μm^2 of cell membrane based on cell capacitance (6.7±0.4 pF; n=28). The number of functional L-type Ca channels was determined using nonstationary fluctuation analysis with whole-cell patch clamp. L-type Ca current was elicited by a 200 msec depolarizing test pulse to +10mV immediately following a 500 msec prepulse to -40mV from a holding potential of -80mV. 100 current records per cell were collected and digitized on-line. Current variance (σ^2) was determined in 20 mM $[Ba^{2+}]_o$ and fitted to $\sigma^2 = iI - I^2/N$. From curve fitting the number of functional L-type channels per cell (N) was 196±26 (n=3) which yielded a channel density of 0.46±0.04/μm^2. From these data the density of DHP receptor sites is greater than 30 times the density of functional L-type Ca channels. The single channel current (i) was -0.23±0.02pA , the peak mean whole-cell current (I_{peak}) was -27.1±2.8 pA and the peak open channel probability (p_{peak}) was calculated to be 0.60±0.02 from $p_{peak} = I_{peak}/Ni$. Supported by NIH HL36059.

3.2

ABNORMALITY IN THE RYANODINE RECEPTOR CALCIUM RELEASE CHANNEL IN HUMAN MALIGNANT HYPERTHERMIA. Thomas E. Nelson. Univ. of Texas Health Science Center, Houston, TX 77030

Malignant hyperthermia (MH) is a pharmacogenetic disease of skeletal muscle predisposing man and animals to an anesthetic-induced, life-threatening syndrome. Abnormal contracture of biopsied human MH muscle exposed to caffeine and halothane and studies on isolated sarcoplasmic reticulum (SR) membranes suggest that abnormal Ca^{2+} release could be involved. To test a hypothesis that Ca^{2+} release channels in SR from human MH skeletal muscle is abnormal, single Ca^{2+} release channels were incorporated from isolated SR membranes into planar lipid bilayers. The effect of halothane on gating and conductance properties, was characterized. In prehalothane controls, mean open time (MOT), mean closed time (MCT) and probability of the channel opening (Po) did not significantly differ between channels from MHS and MHN muscle. Mean amplitude for MHS channels (15.97 pA) was greater than the MHN channels (10.92 pA). Halothane (4-32 μM) had no significant effect on the measured variables of 10 channels from MHN muscle. In 7 of 13 channels from muscle of 5 MHS patients, halothane, 4-32 μM increased Po and MOT while decreasing MCT. Halothane also affected conductance of the MHS channel by changing it from a lower to a higher level. The abnormality of halothane's effect to increase conductance of the single MHS calcium release channel suggests that a mutation in the ryanodine receptor protein is associated with MH susceptibility in man.

3.3

DISCONTINUOUS VOLUME TRANSITIONS IN THE ECTOPLASM AND THE PROCESS OF ACTION POTENTIAL PRODUCTION. Ichiji Tasaki. N.I.M.H. Bethesda, MD. 20892

Phase-transitions involving discontinuous volume changes can be elicited in natural and synthetic polymer gels in vitro by small perturbations of the environment (T. Tanaka, Sci. Amer. 244:110, 1981). Using polycarboxylate gels, we have demonstrated discontinuous volume transitions evoked by varying the concentration ratio of the univalent cations (Li, Na, K, guanidine, etc.) to the divalent cations (Ca, Sr, etc.) in the medium. A transition of gel from a shrunk (Ca-ion rich) state to a swollen (univalent-cation rich) state is an exothermic process; the reverse process is endothermic. For the following reasons, the process of nerve excitation is interpreted as being associated with a phase transition in the ectoplsm. (1) Nerve fibers swell rapidly when excited; the time-course of swelling is similar to that of the action potential and of the rate of temperature rise. (2) Ion mobilities are expected to be profoundly enhanced by swelling. (3) Action potentials can be evoked by lowering the divalent cation concentration in the outside medium. (4) Prolonged action potentials can be prematurely terminated by a heat pulse or 'Ca pulse'. (5) In media containing Mg-ions as the sole divalent cation, the ability of nerve fibers to produce action potentials cannot be sustained; in polycarboxylate gels, discontinuous volume transitions can not be demonstrated by using only Mg and univalent cations. Implications of this interpretation will be discussed.

3.4

SULFHYDRYL-SPECIFIC REAGENTS ACTIVATE A CALCIUM CURRENT AND ENHANCE MECHANICAL RESPONSES IN AN INVERTEBRATE STRIATED MUSCLE. C. Zuazaga, L. Lizardi, M.C. Garcia and J. A. Sanchez (SPON: R. K. Orkand). Inst. of Neurobiology, U. of Puerto Rico Med. Sci. Campus, San Juan, PR 00901.

The effects of the sulfhydryl alkylating agents N-ethylmaleimide (NEM) and 4-cyclopentene-1,3-dione (4-CPD) on current- and voltage-clamped muscle fibers of the crustacean Atya lanipes were examined using two- and three-microelectrode methods, respectively. Control fibers responded completely passively to depolarizing current steps. K and Cl currents underlied these responses since in voltage-clamped fibers the observed currents were blocked by TEA-containing, Cl-free solution; inward cationic currents were not detected. Following exposure to the reagents (2-4 mM), the fibers generate Ca spikes (Zuazaga & del Castillo, Comp. Biochem. Physiol. 82C: 409, 1985). Under voltage-clamp conditions, an inward current which was abolished in Ca-free solution was observed. The induced I_{Ca} was maximal near 0mV, decayed during maintained depolarizations, and was sensitive to nifedipine. Isometric tension was measured on bundles of 15-20 fibers. Tetanic tension was strictly dependent on $[Ca^{2+}]_o$; it increased ca. 300% after 4-CPD. K contractures were produced by isotonic replacement of Na^+ with K^+; peak contracture tension increased after NEM treatment. These results indicate that the reagents activate Ca channels; the increased tension in the chemically-modified fibers is probably due to an increase in Ca^{2+} influx. (Supported by NIH grant NS-07464).

3.5

CHARACTERIZATION OF THE Ca^{2+} ENTRY CHANNEL IN THE BASOLATERAL PLASMA MEMBRANE OF RAT PAROTID GLAND ACINAR CELLS. Timothy Lockwich, Bruce J. Baum, and Indu S. Ambudkar NIDR, NIH, Bethesda, Maryland. Spon: Adil E. Shamoo.

Isolated basolateral plasma membrane vesicles (BLM) from rat parotid glands were used to characterize the putative Ca^{2+} channel which mediates Ca^{2+} entry into the parotid acinar cell. The Ca^{2+} permeability of BLM was determined by monitoring $^{45}Ca^{2+}$ release from actively-loaded (via the Ca^{2+}-ATPase) inside-out BLM vesicles. The data demonstrate that the Ca^{2+} permeability in BLM is modulated by the membrane potential with the fastest rates of Ca^{2+} release occuring upon hyperpolarization of the cytoplasmic side of the membranes. This increased rate of release due to hyperpolarization is blocked by 1 mM Ni^{2+}, but not by agents which block other types of Ca^{2+} channels, e.g. ruthenium red, w conotoxin and heparin. In addition, the Ca^{2+} permeability is regulated by $[Ca]_o$ ($[Ca^{2+}]$ on the cytoplasmic face of the membrane). When $[Ca^{2+}]_o$ is increased above 100nM, the rate of Ca^{2+} release is markedly decreased to a much lower level, which is independent of $[Ca^{2+}]_o$ (200nM-2uM). This effect of $[Ca^{2+}]_o$ on Ca^{2+} release is also independent of the membrane potential and the Ca^{2+} load in the vesicles. The range of $[Ca^{2+}]_o$ in which the BLM Ca^{2+} permeability is regulated in this study is similar to that found in resting and stimulated parotid cells (50-500 nM). In aggregate the data suggest that Ca^{2+} entry into parotid acini is regulated by the cytosolic $[Ca^{2+}]$ and is driven by the electrochemical gradient of Ca^{2+}.

3.6

Na^+ PERMEABILITY CHANGE PREDICTED PROPORTIONAL TO GATING CURRENT. Dexter M. Easton, Dept. of Biological Science, Florida State University, Tallahassee, FL. 32306

The Na^+ current evoked by voltage clamp can be predicted from the assumptions 1) that there is a change in the macroscopic permeability proportional to exponentially decaying fast and slow components of the Na^+ gating current, and 2) that the initial magnitude and rate of decay of these components change at a changing rate, in proportion to the voltage step. The time course of the Na^+ permeability change found from the solution of the differential equations is the product of exponentiated exponential (EE) "activating" and "inactivating" terms, and the V dependence is also EE in form. The equations, with 9 rational constants, and no additional assumptions, permit prediction of any conditioning-testing combination, including prehyperpolarization delay, development and removal of inactivation, and recovery from prolonged inactivation. The equations show the collective results of charge displacements affecting the open state probability within the many channels accessed during macroscopic voltage clamp.

3.7

CONSTANT FIELDS AND CONSTANT GRADIENTS IN OPEN IONIC CHANNELS. R.S. Eisenberg, D.P. Chen, and V. Barcilon, Department of Physiology, Rush Medical College, Chicago IL, 60612.

Ions enter cells through pores in proteins that are holes in dielectrics. The energy of interaction between an ion permeating a pore and the charge induced in the nearby protein should be many kT; in most theories, ion movement depends exponentially on energy, so the dielectric properties of the protein cannot be safely ignored. We describe ionic flux by three dimensional Nernst–Planck equations and potential by Laplace's equation in the pore and protein, allowing space charge and induced charge. Matched asymptotic expansions yield one dimensional approximations to concentration and potential within the channel and the flux and current through the channel.

Classical constant field equations are derived (***not*** assumed) only if the induced charge is small, e.g., if the channel is short or the total concentration gradient is zero. Then, the interaction of ion and channel can be described by a mean potential. If the channel is long, a constant gradient of concentration is derived. The general case is often quite distinct from either constant field or constant gradient—it is easily computed using commercially available programs.

This dielectric theory can easily be tested: its parameters can be determined by traditional constant field measurements. Current voltage relations in other conditions are then predicted without adjustable parameters. For example, the theory predicts current–voltage relations quite different from constant field, usually more linear, when gradients of total concentration are imposed, as in classical measurements of 'dilution' or 'bi–ionic' potentials.

3.8

DOES PHOSPHORYLATION INCREASE THE OPEN PROBABILITY OF CALCIUM CHANNEL OF CARDIAC MUSCLE ? Rikuo Ochi, Takeshi NAKAMURA and Hong-yu Li. Department of Physiology, Juntendo University School of Medicine, Tokyo 113, Japan

Beta-adrenergic stimulants increase Ca^{2+} current of cardiac muscle by decreasing the number of blanks with little change in the open probability (Po) in non-blank sweeps (Ochi & Kawashima, 1990). Maximal phosphorylation of the channel, however, increases Po by favoring the occurrence of the mode 2 sweeps characterized by long open time (Yue, Herzig & Marban, 1990). We recorded single L-type Ca^{2+} channel currents from isolated guinea-pig ventricular cells with the pipettes containing 100 mM Ba^{2+} under cell-attached configuration applying 100ms test steps to 0mV at 2Hz. In the presence of 100 nM BAY K 8644, 1000 nM ISO significantly increased the mean open time from 2.28ms to 3.27 ms, concomitantly increasing the percentage of the sweep with mean open time of longer than 2ms (mode 2 sweep) from 24% to 42%, and increased Po. In the absence of BAY K, strong beta-stimulation with 50μM ISO or 50μM dobutamine (DB) prolonged the mean open time from 0.81 and 0.67ms for controls to 2.00 and 1.06ms for ISO and DB, respectively, both resulting in increase of Po. This effect was mimicked by high dose of 8-Br-cAMP (4mM) or co-application of 2μM ISO and 20μM isobutylmethylxanthine. Thus strong phosphorylation could prolong the open time to increase the open probability of cardiac calcium channel.

3.9

MODELLING OF CARDIAC SODIUM CHANNEL AND THE RELATIONSHIP BETWEEN $\dot{V}_{max}$ AND I_{Na} UNDER PHYSIOLOGICAL CONDITIONS

J. Toyama, T. Anno, A. Taniguchi, M. Shirakawa* and S. Usui* Res Inst of Environ Med, Nagoya Univ, Nagoya, *Dept of Info & Comp Sci, Toyohashi Univ of Tech, Toyohashi JAPAN

A mathematical model was reconstructed based on the upstroke and sodium current separately recorded from enzymatically dispersed ventricular myocytes of guinea pig using the patch clamp technique. The upstroke was induced by the protocol for voltage-dependent inactivation. To calculate the upstroke velocity ($\dot{V}$), an appropriate FIR digital filter was designed. Phase plane plots (membrane potential vs $\dot{V}$) were used for nonlinear parameter optimization of a mathematical model structurally analogous to Hodgkin and Huxley formulation. Our model could reproduce following experimental results: 1) voltage-dependence of availability for $\dot{V}_{max}$, and phase plane plots, 2) activation and inactivation kinetics qualitatively similar to sodium currents at 37°C, 3) the current-voltage relationship and its descending limb over 40 mV (Murray 1990). According to our simulation of voltage-dependent availability for $\dot{V}_{max}$ and I_{Na}, the relationship was fairly linear at 37°C.

3.10

Na^+ CHANNEL ISOTYPES IN ADULT RAT DORSAL ROOT GANGLION NEURONS IDENTIFIED BY ELECTROPHYSIOLOGICAL AND MOLECULAR BIOLOGICAL TECHNIQUES. Caffrey J.M., Brown L.D., Emanuel J.G.R., Eng D.L., Waxman S.G. and J.D. Kocsis. Dept. of Neurology, Yale Univ.Sch.Med., New Haven, CT 06510; V.A. Med.Cntr., W. Haven CT. 16516

Expression of Na^+ currents with distinctive kinetic and pharmacological properties can be correlated with defined size classes of enzymatically-isolated, adult rat dorsal root ganglion (DRG) neurons maintained in short-term primary culture. A single TTX-sensitive Na^+ current ("α-type": V_h= -87.5mV; 6msec > τ_h > 0.4msec) is detectable in outside-out patches excised from large cells ("A-type" neurons: diameter >50μm). Rapidly-inactivating, TTX-sensitive Na^+ current ("β-type": V_h= -85mV; 0.7msec > τ_h > 0.3msec) and slowly-activating and -inactivating, TTX-resistant Na^+ current ("γ-type": V_h= -45mV; 24msec > τ_h > 1msec) are always expressed in small cells ("C-type" neurons: diameter <30μm) as measured in whole-cell current and excised patches. Neurons of intermediate size exhibit current expression either like large (α-type current) or like small neurons (β- and γ-type currents). Action potential properties, Na^+ current densities and kinetics do not change significantly within these defined size classes during the first five days of primary culture. To further define these channels, we are visualizing Na^+ channel mRNA in cultured DRG neurons by *in situ* hybridization histochemistry using PCR-derived, non-radioactively-labeled probes. Correlations between message and channel expression are being established.

3.11

ION CHANNEL PROPERTIES ARE ALTERED BY LIPID BILAYER COMPOSITION.

H.M. Chang (1), S.M. Gruner (2) & R. Gruener (1) Physiol. Dept. Univ. of Arizona, Tucson AZ 85724 (1), Physics Dept. Princeton Univ. Princeton NJ 08544 (2).

Recent evidence has linked membrane lipid composition to function during development and aging, under physiological conditions and in various diseases (review: Yeagle, FASEB J. 3:1833, 1989). We previously reconstituted the rat brain, high-conductance calcium-activated potassium (CaK) channel into PE:PS (1-palmitoyl-2-oleoyl-phosphatidylethanolamine: 1-palmitoyl-2-oleoyl-phosphatidylserine) bilayers (Krueger, Nature 303:172, 1983), with a cis--trans potassium gradient of 300:100 mM, and showed that channel kinetics are not affected when the lipid ratio was varied from 3:7 to 9:1. We concluded, therefore, that surface charge density does not play an important role in ion channel behavior. In contrast, addition of cholesterol, to PE:PS bilayers, resulted in a significant reduction of the mean opentime and the open probability. At the same time, channel conductance remained essentially unchanged. To further study lipid-protein interactions, we reconstituted the CaK channel into bilayers made from 100% dioleoylphosphatidylcholine (DOPC) and 100% monomethylated DOPE (METH-DOPE). The former has a larger spontaneous radius of curvature (SRC) and a higher phase transition temperature (Gruner, S.M.; J. Phys. Chem. 93:7562, 1989). In DOPC membranes, the CaK channel had a longer mean opentime than in METH-DOPE membranes. One possible mechanism for these diverse, lipid-induced actions is the possibility that the position of channel proteins is altered relative to the phospholipids of the bilayer. This effect is likely to result in an altered conformation of the channel, and therefore its ability to go through open/closed transitions. It is expected that membranes made with DOPC would have a lower elastic energy compared to those made from DOPE (Gruner,1989). Similarly, cholesterol has been shown to increase the order parameter of membranes, thus increasing their rigidity (Yeagle, FASEB J. 3.1833, 1989). Our results are consistent with the idea that the lipid composition of bilayers modulates ion channels behavior through changes in their physical environment. Increased membrane rigidity may restrict the ability of channels to undergo conformational changes thus reducing their open time and open probability. In contrast, the reduced elastic energy in DOPC membranes may lower the recoil force of the channel undergoing conformational changes resulting in a longer open time when compared to METH-DOPE membranes.

Supported in part by grants from the Am. Dia. Cntl. Res. Comm. and the BRSG to RG.

3.12

REGULATION OF APICAL EPITHELIAL Na^+ CHANNELS BY ACTIN FILAMENT ORGANIZATION. Adriana G. Prat, Dennis A. Ausiello, and Horacio F. Cantiello. Renal Unit, Massachusetts General Hospital and Dept. of Medicine, Harvard Medical School, Boston, MA 02114.

The functional role of the cytoskeleton in the control of ion channel activity is unknown. In the present study, the patch-clamp technique was used to assess the role of cortical actin networks on apical Na^+ channel regulation in A6 epithelial cells. The fungal toxin and actin filament disrupter, cytochalasin D (5 μg/ml), induced Na^+ channel activity in cell-attached patches within 5 minutes of addition. Cytochalasin D also induced and/or increased Na^+ channel activity in 90% of excised patches tested within 2 minutes. In contrast, no effect was observed with the related compounds cytochalasins A, B or E. Addition of purified G actin (5 μM) to excised patches also induced channel activity. This effect was enhanced by addition of ATP and/or cytochalasin D. The effect of actin on Na^+ channel activity was reversed by addition of the G actin binding protein, DNAse I, or completely prevented by treatment of the excised patches with this enzyme. Addition of short actin filaments in the form of G actin:gelsolin complexes in molar ratios < 8:1, was also effective in activating Na^+ channels. In contrast, addition of the actin-binding protein filamin, which crosslinks actin filaments, reversibly inhibited both, spontaneous and actin-induced Na^+ channels. These data demonstrate a functional role for the cortical actin network in the regulation of epithelial Na^+ channels which may complement a structural role for membrane protein targetting and assembly.

3.13

ION CHANNEL REGULATION BY A CYTOSKELETAL-ELECTRODYNAMIC NETWORK. Horacio F. Cantiello and Deak S. Kim. Renal Unit, Massachusetts General Hospital and Department of Medicine, Harvard Medical School, Boston, MA 02114.

The role of actin filament organization in the control of ion channels (FASEB J. 5:A690, 1991) and the conduction of electrical currents (Biophys. J. 59: in press), has been recently established in our laboratory. In this report we describe the use of "chopstick" or double, cell-attached patch-clamp configuration on A6 epithelial cells to assess the role of intracellular actin networks on the control by electrical coupling of ion channels from various localized plasma membrane domains. Electric fields, V_f, applied onto an average membrane area ~3 μm^2, elicited ion channel activity on another cell location > 5 μm away from V_f. Ion channel activation depended on the polarity of V_f and was vectorially oriented. Three criteria were established to determine that membrane coupling between electric field induction and the site of collection was mediated by the cytoskeleton: 1) coupling was observed in the presence of 1-5 mM $LaCl_3$ to screen surface charges; 2) coupling was observed after cell-permeabilization with saponin; and 3) coupling between two excised, inside-out, patches in free solution was re-established by addition of actin and ATP. The data indicate that actin-based networks serve as a novel electrodynamic intracellular network able to conduct locally-established electric field fluctuations at the plasma membrane level. This cytoskeletal coupling of cell membranes may play an important role in the onset of cell polarity and development.

3.14

PURIFICATION OF CARDIAC MYOCYTE CULTURES FOR USE IN CALCIUM CHANNEL EXPRESSION STUDIES. **Andrew Lokuta, W.J. Lederer, and Terry B. Rogers.** University of Maryland Medical School. Baltimore, MD 21201

A popular model for mammalian heart in biochemical research is the neonatal rat cardiac myocyte culture. Several research groups are currently investigating molecular changes in these myocytes that occur after exposure to peptide growth factors. Our lab is particularly interested in possible changes in calcium channel expression after adding angiotensin II or thyroid hormone to the cultures. A potential problem we recognized was the heterogeneity of the neonatal rat heart preparation. Serum-free supplements, mitotic inhibitors, and gamma irradiation were all tested as a means to reduce nonmyocytes while still maintaining healthy functional myocytes. Protein levels, spontaneous beating rates, and the amount of PAS-positive staining material were all used as indices of myocyte quality when different interventions were tried. The data suggests that gamma irradiation is the optimal method to reduce nonmyocytes and yet maintain viable myocytes. This work serves as the basis for the next step in addressing the issue of growth factor induced changes in calcium channel expression. For example, using this purification method, preliminary experiments suggest that angiotensin II increases dihydropuridine binding sites.

3.15

SINGLE-CHANNEL KINETICS OF NMDA RECEPTORS IN *XENOPUS* SPINAL NEURONS. Yinong Zhang and Anthony Auerbach. Department of Biophysical Sciences, SUNY at Buffalo, Buffalo, NY 14214

Using cell-attached patches, we have studied the effects of changing [NMDA], $[Mg^{+2}]$ and membrane potential on the kinetic properties of NMDA channels in embryonic *Xenopus* spinal neurons. The data were fitted to a 5 state model:

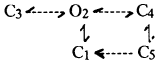

where C_1 is vacant-closed, O_2 is liganded-open, C_4 is liganded-blocked (by Mg^{+2}), C_5 is vacant-blocked (i.e., Mg^{+2} trapped) and C_3 is a long lived closed state. We used Horn and Lange's maximum likelihood method of analysis. k_{24} is increased by hyperpolarization and $[Mg^{+2}]$ but is unaffected by [NMDA]. k_{12} increases with increasing [NMDA] but is insensitive to Mg^{+2} and only slightly voltage dependant. k_{21} is independent of both NMDA and $[Mg^{+2}]$ but slows somewhat with hyperpolarization. Preliminary results indicate that at -90mV the maximum channel opening rate(k_{12}) is about 325 s^{-1}, and Mg^{+2}blocks channels(k_{24}) at a rate about $3.7x10^8$ s^{-1} M^{-1}.

We have tested other kinetic schemes and have found none that fit the data better than the one shown above, where each state of the model has a clear physical correlate.

Supported by grants from NIH and NSF to A.Auerbach.

3.16

PROPERTIES OF ENDOGENOUS VOLTAGE-DEPENDENT NA CHANNELS IN XENOPUS OOCYTES. Douglas S. Krafte and Walter A. Volberg. Department of Cardiovascular Pharmacology, Sterling Research Group, Rensselaer, NY 12144. (Sponsor - E. Pagani).

Xenopus laevis oocytes have been widely used as an expression system for the study of ion channels. Endogenous currents in the oocyte have been well characterized and, in most cases, do not represent a significant source of contaminating current when studying exogenous channels. Here we report the properties of an endogenous, voltage-dependent Na channel that is present in < 5% of the batches of oocytes studied. This channel differs from a previously reported oocyte Na channel which activates at very depolarized potentials (> +20 mV). In one batch of oocytes from a single donor, the endogenous Na currents were sufficiently large for quantitative study. Average peak current amplitudes were -279 ± 17 nA at -10 mV which was the peak of the current-voltage relationship. Steady-state inactivation assessed with 100 ms prepulse protocols occurred with a V1/2 of -38 ± 0.5 mV and a slope factor of 7.6 ± 0.3 / mV. The channels were blocked by tetrodotoxin in a dose-dependent manner with an IC50 value of 6 nM. Endogenous Na currents showed significant attenuation of peak current amplitude when stimulated at 10 Hz with a > 30% reduction in amplitude during a 30 pulse train. The properties of these endogenous channels are distinct from channels expressed following injection of exogenous neuronal or cardiac RNA. The fact that endogenous Na channels can be present in the oocyte membrane, however, underscores the necessity for a careful examination of control oocytes from different donors.

3.17

FREQUENCY-DEPENDENT EFFECTS OF SEA ANEMONE TOXINS ON REFRACTORINESS AND ACTION POTENTIAL DURATION - LACK OF CORRELATION WITH EFFECTS AT CARDIAC SODIUM CHANNELS. **G.M. Briggs, D. Krafte, P. Canniff, W. Volberg, and A. Ezrin. Department of Cardiovascular Pharmacology, Sterling Research Group, Rensselaer, NY 12144. (Sponsor - A. Buchholz)**

Sea anemone toxins (ATX II, AP-A) have been shown to act at voltage-dependent Na channels to slow inactivation and prolong refractoriness in vivo. The increase in refractoriness is frequency-dependent and effects are most pronounced at slow stimulation rates. We have investigated the effects of these toxins in whole hearts, isolated ventricular tissue, and expressed Na channels to determine whether the frequency-dependence of toxin activity can be explained by actions at the Na channel. In isolated Langendorff hearts 10 nM AP-A produced a 300 ms increase in refractoriness with an associated increase in dP/dt of 80% at a pacing rate of 1 Hz. When the rate was increased to 3.3 Hz, however, refractory periods and dP/dt were not different from control. In isolated ventricular tissue similar frequency-dependent effects were seen on action potential duration. At 0.5 Hz APD was increased by 100% by 10 nM ATX II while at 2 Hz APD was increased by 10%. Frequency-dependent actions on Na channels were examined by measuring the effects of AP-A or ATX II on cardiac Na currents expressed in oocytes. Change in Na current integrals was used to assess activity for the 1st and 30th pulses in a 10 Hz train. No differences were found when comparing the first and last pulses indicating no use-dependent effect at 10 Hz. These data suggest other channels may be responsible for the frequency-dependent changes in refractoriness and APD during exposure to these toxins.

3.18

CALCIUM CHANNEL MODULATION BY NOREPINEPHRINE AND GABA. Daniel H. Cox and Kathleen Dunlap, Physiology Department, Tufts Medical School, Boston, MA 02111

GABA and norepinephrine (NE) inhibit high voltage activated (HVA) calcium current in dorsal root ganglion neurons. We have employed ω-conotoxin (ω-CgTx) and a dihydropyridine (DHP) agonist, (+)-(s)-202-791, and antagonist, nimodipine, to 1) characterize the HVA currents in the neurons and 2) determine which channel type is modulated by the transmitters. ω-CgTx (9 μM) blocks irreversibly virtually 100% of whole cell HVA calcium current in acutely dissociated neurons from 12 day old ganglia. This ω-CgTx-sensitive current shows a rather shallow steady-state inactivation curve, with an e-fold change produced by a 10 mV shift in holding potential and a half-maximal inactivation at -53 mV. It is also characterized by both readily inactivating and slowly inactivating components. Over time, ω-CgTx-resistant current increases to ca. 15% of total HVA current by day 6 *in vitro*. This current component is inhibited entirely by nimodipine (5 μM). The calcium channel agonist (+)-(s)-202-791 (2 μM) not only enhances the ω-CgTx-resistant current but also prolongs the tail current following repolarization, generating a means by which the two components of HVA current can be separated in the absence of antagonists. ω-CgTx does not inhibit this prolonged tail, indicating that the toxin is selective for the DHP-resistant (or N-type) current. GABA and NE modulate the ω-CgTx-sensitive component of the current as evidenced by their lack of effect on 1) the ω-CgTx-resistant current and 2) the (+)-(s)-202-791-prolonged tail current. Thus, the transmitters appear to specifically modulate the N-type and not L-type calcium current in dorsal root ganglion neurons.

3.19

TENSION SENSITIVITY OF ALAMETHICIN CHANNEL CONDUCTANCE STATE DISTRIBUTION AND KINETICS L.R. Opsahl, W. W. Webb* Spon: G.W.G. Sharp**. Dept of Physics, School of Applied and Engineering Physics*, and Dept of Pharmacology**, Cornell U., Ithaca, NY

Alamethicin in lipid bilayers assembles into multisubunit ion channels which switch amongst several conductance states. We have used single channel recording to measure the effect of membrane tension, t, on the relative occupation probabilities P_i of the various states of alamethicin and have used event detection to obtain kinetic information from the single channel data. An increase in t results in an increase in the P_i of higher conductance states relative to lower conductance states. Using Boltzman statistics we show that the relative equilibrium occupation probabilities of states i and j are related to the difference in area occupied, $A_i - A_j = \Delta A_{ij}$ and membrane tension t by $ln(P_i/P_j) = -(G_o - t\Delta A_{ij})/kT$, where G_o is independent of t. We have found that the change in effective cross sectional area of the alamethicin channel when switching between adjacent conductance states is consistent with an area change associated with the incorporation of a helical monomer into the phospholipid membrane. In order to further clarify the structural changes involved in channel gating, we have done kinetics analysis on our single channel data. Multiple conductance state event detection is used to produce dwell time histograms which represent the probability distribution functions for the conductance levels. We have found that the probability distribution functions are linear superpositions of at least two exponential functions which implies that there are multiple conformational states for each conductance level.

3.20

MUTATIONAL EFFECTS AND FUNCTIONAL ROLE OF IONIC CURRENTS IN "GIANT" *DROSOPHILA* NEURONS.
M. Saito and C.-F. Wu. SPON: K. Campbell, Department of Biology, University of Iowa, Iowa City, IA 52242

Complex patterns of neuronal activity are derived from interaction among various inward and outward currents. One way to investigate mechanisms of neuronal activity is to study the functional alterations of single gene mutations that affect individual currents in *Drosophila*. Because of the small size of *Drosophila* neurons, the role of each membrane current has not been well studied. We used "giant" *Drosophila* neurons, derived from cell-division arrested neuroblasts, to examine the role of and effects of mutations on neuronal currents by correlating voltage- and current-clamp results in the same cell. We have observed in these neurons Na and Ca inward currents, and K outward currents, i.e. voltage-activated I_A and I_K and Ca-dependent $I_{K,Ca}$. In addition, we found a persistent Na current ($I_{Na,P}$) and a TTX sensitive Na-dependent K current ($I_{K,Na}$). I_A is known to control inter-spike intervals and to delay action potential initiation. However, we observed variation in I_A properties. In some neurons, I_A inactivated at more positive potentials, suggesting possible involvement in action potential repolarization. Manipulating I_A inactivation by changing resting potential did not alter action potential durations in wild-type neurons, because of the presence of $I_{K,Ca}$. But the same manipulation broadened spike duration in neurons from *slowpoke*, a mutant with defective $I_{K,Ca}$. This confirms that both I_A and $I_{K,Ca}$ contribute to action potential repolarization. The role of $I_{Na,P}$ and $I_{K,Na}$ in the regulation of spike discharge pattern was suggested by ion replacement experiments. Li permeates the Na channel but does not activate $I_{K,Na}$. Li in place of Na reduced afterhyperpolarization, and induced cumulative depolarization during repetitive firing.

3.21

RAS INDUCTION OF SODIUM CHANNELS IN MEDULLARY THYROID CARCINOMA CELLS. S.A. DeRiemer[1], B.D. Nelkin[2], H. Tamir[3]. Spon: S. Silverstein. Depts of Biol. Sci.[1] & Anatomy and Cell Biol.[3], Columbia Univ., NY NY 10027; Oncology Ctr.[2], Johns Hopkins Med. Inst., Baltimore, MD 21205.

Human medullary thyroid carcinoma (MTC) cells are derived from the calcitonin secreting parafollicular cells of the thyroid. These cells, like other neural crest derived cells, can be induced to exhibit neuronal properties including a vesicular serotonin binding protein and the synthesis, storage and release of the neurotransmitters CGRP, serotonin, and somatostatin. In order to further the comparison of MTC cells with neurons, and to study the mechanisms of phenotypic switch, we have used the whole-cell patch clamp to measure ionic currents in MTC (TT) cells and in cells infected with Harvey Murine Sarcoma Virus (HaMSV) containing the Ha-ras oncongene plus the 1504 Helper Virus. Cells infected only with the Helper Virus served as controls. Infected cells showed increased expression by immunocytochemistry of neurofilaments. On several occasions, infection caused expression of NGF receptor and addition of NGF led to neuritic outgrowth. The two major currents observed in the MTC cells were a TEA-sensitive delayed rectifier and a small, non-inactivating calcium current. These two currents were both present in the HaMSV and Helper infected cells. The major difference observed in the HaMSV cells was a prominent TTX-sensitive sodium current which was absent from the two sets of controls. Unlike the MTC (TT) cell line, freshly plated MTC tumor cells have sodium action potentials (Sand, et al., 1986). These results suggest that the expression of sodium channels can be down regulated upon establishment of cell lines and restored or induced by the G-protein like ras gene. .

Support was from NSF (DCB-86-15840) to SAD; NIMH (MH-37575-2HT) to HT.

3.22

STRETCH ACTIVATION OF THE S CHANNEL IN MECHANOSENSORY NEURONS OF APLYSIA. D.H.Vandorpe & C.E.Morris. Neurosciences, Loeb Institute, Ottawa Civic Hospital, Ottawa, Canada K1Y 4E9

In molluscan neurons, stretch-activated (SA) K channels do not seem to be physiologically mechanosensitive (Morris & Horn 1991 Science 251:1246). What, then, is their true modality? Molluscan SAK channels share many features with a receptor-mediated channel, the serotonin (5HT) sensitive K channel of Aplysia mechanosensory neurons (the S-channel). We demonstrate, using cell-attached patches, that the S-channel is a SAK channel. Bath application of 100 μM 5HT significantly decreased the activity of spontaneously active channels which could subsequently be reactivated by stretch. 20 μM FMRFamide activated quiescent (and stretch-activatable) S-channels. The features of a receptor-mediated channel that would make it suseptible to membrane tension under single channel recording conditions are unknown.

Supported by NSERC, Canada.

3.23

CHARACTERIZATION OF ATP-REGULATED K^+ CHANNELS IN HUMAN AIRWAY EPITHELIA. J. Gregory Fitz, J.R. Yankaskas, and M. Jackson Stutts. SPON: C. William Davis. Duke Univ., Durham, N.C. 27710, and Univ. of North Carolina, Chapel Hill, 27514.

Activation of Cl- channels in airway epithelia leads to Cl- secretion and membrane depolarization, but the mechanisms responsible for compensatory K+ efflux and cellular repolarization are not well defined. Using patch clamp techniques, we have identified K+ selective ion channels in differentiated epithelial cell lines derived from airways of normal and CF patients. **RESULTS:** K+ selective channels with a unitary conductance of 110-130 pS and P_{Na+}/P_{K+} ~.05 were present in both cell-attached and excised membrane patches. Open probability (P_O) was Ca^{2+} -insensitive, but increased with depolarization from 0.03± .02 at 0 mV to .28 ± .09 at -40 mV. P_O was unaffected by the K+ channel blocker TEA (4 mM) but was increased by diazoxide (200 uM, 4/5). ATP (cytoplasmic face) had reversible and dose-dependent effects, increasing P_O at concentrations <0.1 mM, but decreasing P_O at concentrations >0.5 mM. The inhibitory effects of ATP were blocked by ADP. **SUMMARY AND CONCLUSIONS:** Airway epithelia have a high conductance K+ channel sensitive to both voltage and intracellular ATP. The physiologic function is not known, but following apical Cl- secretion, K+ channel activation may contribute to cellular repolarization and prevent intracellular accumulation of K+ related to increased Na+/K+ pump activity.

3.24

REGULATION OF CHLORIDE CHANNELS IN HUMAN SKELETAL MUSCLE. Ch. Fahlke, E. Zachar and R. Rüdel (SPON:M.Morad). Department of General Physiology, Univ.of Ulm, D-7900 Ulm, Germany.

The Cl^- channels in human myoballs were investigated with a combination of whole-cell and single-channel-recording. The whole-cell measurements showed two Cl^- current components active at the resting potential, one with activating kinetics upon voltage jumps in positive direction, the other with inactivating kinetics. Two corresponding Cl^- channels were characterized in single-channel measurements.

The activating whole-cell current became more prominent the longer the experiment lasted, suggesting that physiological regulating substances might be washed out by dialysis through the pipette. The regulation of the Cl^- channels was therefore investigated with whole-cell recording, occasionally through patches perforated with *staphylococcus* α-toxin. Extracellular application of a protein kinase C activating phorbol ester (phorbol 12-myristate 13-acetate) lead to a decrease of the activating and an increase of the inactivating Cl^- current component within 30 min. The action of the phorbol ester was prevented either by intracellular GDP-β-S or by the specific kinase C blocker H8, but not by intracellular pertussis toxin. Decrease of the activating and increase of the inactivating Cl^- current components were also seen after intracellular application of GTP-γ-S, even when protein kinase C was blocked by H8. These results could indicate that protein kinase C affects the Cl^- channels via a regulating G protein system. Supported by DFG (Ru 138/17).

3.25

Voltage-sensitive and Solvent-sensitive Processes in Ion Channel Gating: Effects of Osmotic Stress on Crayfish Sodium Channels. M.D. Rayner and J.G. Starkus, SPON: G.C. Whittow. Department of Physiology and Békésy Laboratory of Neurobiology, University of Hawaii, Honolulu, Hawaii 96822

Effects of osmotic stress on sodium ionic and gating currents have been studied in crayfish giant axons after removal of fast inactivation with chloramine-T. Internal perfusion with media made hyperosmolar by addition of formamide or sucrose, reduces peak sodium current in a voltage-independent manner. Equilibrium data closely parallel the results obtained by Zimmerberg et al. (1990 *Biophys. J* 57:1049-1064) for delayed rectifier potassium channels. For sodium channels also, increased hydration of the channel protein appears necessary for channels to enter into their conducting state.

Additionally, exposure to hyperosmolar perfusates slows sodium current activation without affecting: a) tail current deactivation rate, b) the kinetics of ON and OFF gating currents or, c) the secondary activation rate following brief interpulse intervals. These results provide further support for separation of channel gating into distinct voltage-sensitive and solvent-sensitive gating processes as proposed by Zimmerberg et al. However our kinetic observations are incompatable with models in which these gating processes are presumed to be either strictly sequential or parallel and independent. We introduce a variant of the parallel model which presumes electrostatic coupling between voltage-sensitive and solvent-sensitive gating mechanisms. Simulations demonstrating the characteristic kinetic properties of our hyperosmolar data can be obtained for coupling energies as small as ~ 1/20th of kT. Supported by PHS grant #NS251151-04, NIH RCMI grant #RR03061 and American Heart Association, Hawaii Affiliate.

3.26

CALCIUM-SENSITIVE CHLORIDE CURRENTS IN VASCULAR SMOOTH MUSCLE CELLS. C. Roger White, Tommy A. Brock and Richard L. Shoemaker. University of Alabama at Birmingham, Birmingham, Alabama 35294.

The following experiments were performed to study mechanisms underlying VSMC chloride (Cl^-) channel activation. We have identified a Cl^- channel (conductance = 25 pS) whose open state probability is dependent on $[Ca^{2+}]$ in excised membrane patches. We also found that angiotensin II (Ang II, 10^{-7} M) stimulates outward Cl^- currents in cell-attached patches. These data suggest that Ang II may stimulate Cl^- channel activity via increases in $[Ca^{2+}]_i$. Subsequent experiments were designed to study the effect of Ca^{2+}-mobilizing agonists, Ang II and ATP, on transmembrane ^{125}iodine (^{125}I) efflux in cultured VSMCs. Both agonists induced rapid increases in ^{125}I efflux rates which were completely abolished after brief incubation (40 μM, 20 min) with BAPTA/AM, a membrane-permeable Ca^{2+}-chelator. However, when EGTA was used to blunt agonist-stimulated Ca^{2+} influx, ^{125}I efflux was still increased in response to Ang II and ATP. These data suggest that the release of Ca^{2+} from intracellular sites is adequate to increase Cl^- channel activity in response to Ang II and ATP.

3.27

UNITARY BUT NOT MACROSCOPIC CONDUCTANCE OF HUMAN CONNEXIN43 GAP JUNCTION CHANNELS IS ALTERED BY PHOSPHORYLATING TREATMENTS. A.P. Moreno, G.I. Fishman and D.C. Spray. SPON: M.V.L. Bennett Albert Einstein College of Medicine. Bronx NY 10461.

Gap junctions participate in the electrical propagation of signals between excitable cells (heart and some neurons) as well as in intercellular diffusion of second messenger molecules including IP_3 and Ca^{++}. Connexin43 is a phosphoprotein that forms gap junction channels between heart cells, between astrocytes, and elsewhere. In order to study the effects of phosphorylation on its physiological properties of specific types of gap junction channels, we have stably transfected SKHep1 cells (a communicating-deficient and highly metastatic human hepatoma cell line) with cDNA that encodes human connexin43. Using a dual voltage clamp method on freshly plated pairs of cells, we measured macroscopic junctional conductance (g_j) and single channel conductance (γ_j) after perfusion of 2 mM halothane which reversibly reduces g_j. In control pairs (n=10 cells, >100 events in each), two unitary conductances were clearly distinguished (60 and 90 pS). After phosphorylating agents were applied (cAMP [cyclic adenosine monophosphate], TPA [tumor promotor phorbol esters], forskolin or okadaic acid), g_j never changed more than 5% (n=3/treatment) but γ_j shifted toward the low conductance state. Staurosporine, which inhibits kinase activation, shifted the distribution towards the higher γ_j value without changing g_j. These results raise the possibility that phosphorylation might modify the selectivity of the gap junction channels to molecules of larger size without changing the strength of electrical coupling between the cells.

3.28

REGULATION OF L-TYPE Ca^{2+}-CHANNELS IN SKELETAL MUSCLE BY cAMP-DEPENDENT PROTEIN KINASE. Adrian Sculptoreanu, Todd Scheuer, William A. Catterall. SPON: Ghassan Bkaily*. Dept of Pharmacology, U. of Washington Seattle, WA 98195. *Dept. Physiol. Biophysics, U. of Sherbrooke, Sherbrooke, Quebec J1H 5N4.

The regulation of cardiac L-type Ca^{2+}-channels by PKA is well characterized. There is little electrophysiological data on the regulation of mammalian skeletal muscle L-type Ca^{2+}-channels. Using whole cell voltage clamp technique we examined the L-type Ca^{2+}-channels of rat skeletal muscle myoballs and their regulation by PKA. With intracellular Cs^+-solution containing ATP and GTP and 10 or 20 mM extracellular Ba^{2+} or Ca^{2+}, DHP-sensitive L-type Ca^{2+}-currents were recorded which ranged between 200 pA and 2 nA. Forty to 60% of this current rapidly runs down within 10 min. of establishing whole-cell configuration; the remainder of the current runs down more slowly. Intracellular addition of the protease inhibitor leupeptin effectively prevented the initial phase of rundown. Dialysis with ATPγs also prevented the initial rundown and in addition produced a 10-20% increase over the initial current. Forskolin, 8-Bromo-cAMP and isoproterenol produced a 50 to 80% increase of L-type Ca^{2+}-current above the ATPγs stimulated current. In the absence of ATPγs, stimulation of PKA produced less dramatic increases in L-type Ca^{2+}-currents.It appears, therefore that regulation of skeletal muscle L-type Ca^{2+}-channels by PKA has aspects that are similar to that reported for cardiac Ca^{2+}-channels.

A.Sculptoreanu is a fellow of the Heart and Stroke Foundation of Canada.

3.29

ACETYLCHOLINE ACTIVATES A CHLORIDE CONDUCTANCE IN MAMMALIAN TRACHEAL MYOCYTES. L. J. Janssen and S. M. Sims. Dept. of Physiology, Univ. Western Ontario, London, Canada, N6A5C1.

We investigated the mechanisms of cholinergic excitation in airway smooth muscle cells isolated from canine and guinea-pig trachealis. Using perforated patch recording, cells were voltage clamped at -60 mV. Acetylcholine (ACh) elicited inward current (I_{ACh}) that peaked and returned to baseline within ≈ 5 s. The cells also contracted, even when voltage clamped and in some cases in Ca^{2+}-free medium, suggesting that Ca^{2+} is released from internal stores. The voltage-dependence of I_{ACh} was studied using voltage ramp commands. I_{ACh} reversed direction at about -20 mV, suggesting I_{ACh} arises due to a mixed conductance. To eliminate a possible contribution of Na^+, extracellular Na^+ was replaced by N-methyl-D-glucamine. ACh still elicited inward current (though smaller than in the presence of Na^+) which reversed direction close to E_{Cl} (≈ 0 mV with symmetric [Cl^-]). Reintroduction of Na^+ increased I_{ACh} and shifted the reversal potential back towards -20 mV. When E_{Cl} was altered using aspartate in the recording electrode, I_{ACh} shifted in a manner predicted for a Cl^- conductance; the shift was greater in the absence of Na^+. The chloride channel blockers niflumic acid or SITS reversibly antagonized I_{ACh}. We conclude that in canine and guinea-pig tracheal smooth muscle, ACh causes contraction and activates a Cl^- conductance as well as a non-selective cation conductance.

These studies were supported by the Canadian Lung Association (Fellowship to L.J.J.) and the Medical Research Council of Canada.

3.30

SUPERSENSITIVITY TO TETRODOTOXIN AND LIDOCAINE OF SEA ANEMOME TOXIN II-MODIFIED Na CHANNELS IN GUINEA-PIG VENTRICULAR MUSCLE. Matomo Nishio, Tsuyoshi Ohmura, Shigeru Kigoshi and Ikunobu Muramatsu. Department of Pharmacology. Fukui Medical School, Matsuoka, Fukui 910-11, Japan.

Sea anemone toxin II (ATX II, 20–30 nM) doubled the action potential duration of the guinea-pig papillary muscles without affecting the maximum rate of rise of action potential ($\dot{V}$max) and the resting potential. The prolonged action potential was shortened by the addition of tetrodotoxin and lidocaine at concentrations (30 nM – 3 μM) where these drugs did not suppress the $\dot{V}$max. The IC_{50} values were approximately 1 μM for tetrodotoxin and 100 nM for lidocaine. On the other hand, the maximum rate of rise of action potential in ATX II-treated and -untreated papillary muscles was not inhibited by such concentrations of each drug; the IC_{50} values of tetrodotoxin and lidocaine were approximately 10 μM and 30 μM, respectively. Whole-cell voltage clamp experiments with single ventricular cells showed that ATX II produced the slowly decaying inward Na current following a transient inward Na current upon depolarization. The slowly decaying current was reduced by tetrodotoxin or lidocaine at the concentrations (300 nM – 1 μM for tetrodotoxin, 3 – 10 μM for lidocaine) where these drugs failed to affect the $\dot{V}$max in the ATX II -untreated cells. These results suggest that Na channel modification by ATX II not only changes its kinetics but also increases the susceptibility of the channels to block by tetrodotoxin and lidocaine.

3.31

SIMULATION OF THE ROLE OF WATER IN ION CHANNEL GATING

Michael E. Green, Department of Chemistry
City College of CUNY, New York, NY 10031

Water in narrow channels behaves differently from water in bulk; water in high electric fields behaves differently from water in low fields. The combination of high fields and very small volume found in ion channels will lead to water structured quite differently from water in bulk. It is hypothesized that this water will block the passage of ions (1), leading to a closed channel. Two types of ions should be able to pass at least part way through: H^+ and OH^-. For these ions, the mechanism of transport is quite different. If these ions neutralize charges on the protein the water would be freed to move, and with it ions such as Na^+ and K^+. Monte Carlo simulation of the water, using a simple water-water potential (TIP4P) supports this hypothesis; energy, orientation of water dipoles, and rate of passage of the water molecules through the end of a tapered channel model, in which a cylinder narrows through a cone to a small opening, have been determined as a function of charge, and all responded as expected(1). Further work, using a water-water potential which includes polarization of the water molecule, will be reported, along with preliminary results with H^+ and OH^- ions.

(1) M. E. Green and J. Lewis (1991) Biophys. J. **59**,419-426

3.32

A Ca^{2+} CHANNEL WITH SMALL CONDUCTANCE AND BAY K 8644 SENSITIVITY IN CAPILLARY ENDOTHELIAL CELLS. A. Feltz, J.-L. Bossu, A. Elhamdani, F. Tanzi, CNRS, F-67087 Strasbourg.

Isolated bovine capillary endothelial cells have been examined for voltage-dependent calcium entry. All cells displayed a low threshold activity, with the main characteristics of a T-type transient current, when examined using whole-cell recording for activation and inactivation and cell-attached conditions or inside-out patches for the elementary conductance (8 pS). 25% of the cells displayed, in 5 mM $CaCl_2$, above -40 mV, an additional sustained current, enhanced by application of BAYK8644, but almost insensitive to nicardipine. Of the two types of channels (2.8 and 21 pS, in 110 mM $BaCl_2$) found on those cells to have a BAYK8644 sensitivity, the large conductance channels were of L-type (with mean open times of 1.8 and 7.8 ms and abolished by nicardipine). The smaller events were elicited at consistently more hyperpolarized potentials (30 mV). Their mean open time was 16 ms in control conditions with additional long openings (mean: 43 ms) in presence of 10^{-6} M BAYK8644. We refer to these channels as SB channels: of small conductance and sensitive to BAYK8644 (above 10^{-8} M). Open times of SB channels are not noticeably modified in the presence of nicardipine when it is added either to control solution or after a BAYK8644 application. At physiological concentrations of divalent ions, an SB-type activity is elicited above -40 mV which generates a low threshold sustained current. A possible functional link between SB- and L-type channels is discussed.

3.33

Ca^{2+}-dependent facilitation and inhibition of the $GABA_A$ response in cultured porcine melanotrophs.

Didier Mouginot, Paul Feltz and Rémy Schlichter. Institut de Physiologie et de Chimie biologique, 21 rue Descartes STRASBOURG cédex

The modulatory role of intracellular calcium concentration ($[Ca]_i$) on $GABA_A$ gated Cl^- currents was investigated in cultured porcine pituitary intermediate lobe (IL) cells using the whole-cell recording (WCR) and the cell attached (CA) recording configurations of the patch clamp technique.

In the WCR configuration, activation of voltage-dependent inward calcium currents did not inhibit the $GABA_A$ receptor mediated response. When the resting $[Ca]_i$ was set at 10^{-7}M, 3Me-His^2-TRH (50nM), a potent analog of Thyrotropin-releasing-hormone (TRH) which activates phospholipase C in our model induced a 40±8% potentiation of the $GABA_A$ gated Cl^- current. This effect was blocked by a high concentration of EGTA (18mM) in the pipette solution, suggesting that this potentiation was mediated by a rise in $[Ca]_i$. In the absence of EGTA in the pipette, either facilitory or inhibitory effects of 3Me-His^2-TRH were observed.

In the CA configuration, the activity of these single $GABA_A$ receptor gated Cl^- channels was reversibly inhibited by application of 3Me-His^2-TRH.

We conclude that a rise in $[Ca]_i$ modulates the $GABA_A$ response in porcine melanotrophs. However, this modulation is only observed when Ca^{2+} is released from intracellular stores, but not during Ca^{2+} influx through voltage operated Ca^{2+} channels.

3.34

ON ION SELECTION IN CA CHANNELS

H.D. Lux, Dept. of Neurophysiology, Max-Planck-Institute for Psychiatry, 8033 Planegg-Martinsried, FRG

The dependence of Ca channel conductance on external $[Ca^{2+}]_o$ shows millimolar Ca^{2+} binding equilibria. However, micromolar $[Ca^{2+}]_o$ blocks the large permeability of the channels for Na and other monovalent cations. At effective blocker concentrations the shift of the activation-voltage curves were small suggesting external binding sites of low affinity for bivalent cations. Relaxation times of block and unblock of Na^+ currents were measured on step changes to and from membrane potentials at which pronounced block occurred as induced by Ca^{2+} and Mg^{2+} ions. The Na^+ currents were unblocked with time constants (τ_u) of 230 to 320 μs at 21°C. τ_u showed a Q_{10} of 2.5 and failed to show obvious dependence on $[Ca^{2+}]_o$ or $[Mg^{2+}]_o$, i.e. to depend on $[Ca^{2+}]_o$ or $[Mg^{2+}]_o$ up to the millimolar range. The blocking time constants decreased with micromolar increase in $[Ca^{2+}]_o$ in line with a blocking rate coefficient of 1.9×10^8 $M^{-1}s^{-1}$ but settled to values near 200 μs for $[Ca^{2+}]_o > 50$ μM. The kinetic features of block and unblock suggest ion specific but concentration independent transitions between configurations with different ion selectivities occurring at a centrally located channel site. State models which reproduce the voltage- and ion-dependent behaviour of the channel demand a blocking conformation that separates the conductive ones. The resulting separation in time of Ca^{2+}, Na^+ and nonconductive states is displayed in the single channel flicker studied in low voltage activated Ca^{2+} channels.

3.35

THE SYNERGISM OF CALCIUM- AND CHLORIDE- CHANNELS IN CHARACEAE. *P.R. Andjus, *D. Vučelić, A.A. Kataev, A.A. Alexandrov and G.N. Berestovsky. *Inst. Gen. Phys. Chem., 11000 Belgrade, Yugoslavia; Inst. Cell Biophys., Pushchino, Moscow Region, 142292 USSR

The giant algal cell of *Characeae* generates action potentials in response to depolarization. This experimental model ("green axon") was used to investigate D_2O-induced excitation. In the perfused plasma membrane under voltage clamp, substitution of D_2O for H_2O generated an inward current. An early Ca^{2+}- and a later, larger Cl^-- current component were identified. The temperature dependence of the D_2O-induced current revealed a narrow peak at 31°C resembling a discontinuity previously reported for water transport. Blocking of Ca^{2+} channels inhibited D_2O-induced excitation. Ca^{2+} channels reconstituted in BLMs were also activated by D_2O. Thus, a Ca^{2+}-dependent Cl^- channel was operational, as in electrical excitation, but, contrary to the case in H_2O, Cl^- channel activation by Ca^{2+} in D_2O was reversible. Dimethylsulfoxide also activated Ca^{2+} channels in BLMs. It is suggested that H-bonded water bridges keep the channel subunits in a functional (open) state.

6.1

REGULATION OF THE CARDIAC α_1 CALCIUM CHANNEL SUBUNIT BY SKELETAL MUSCLE β AND γ SUBUNITS

Xiangyang Wei, Edward Perez-Reyes, Antonio Lacerda, Lutz Birnbaumer, and Arthur M. Brown* Baylor College of Medicine, Houston, Texas 77030

L-type calcium channels are thought to consist of a complex of α_1, α_2-δ, β and γ subunits. Expression of the cloned α_1 subunit from skeletal and cardiac muscle has established that this protein is the dihydropyridine-sensitive ion conducting subunit. The other putative subunits have been postulated to modulate both the response of α_1 to phosphorylation and its activation kinetics. To determine the modulatory roles of these putative subunits we have cloned a full-length cDNA encoding the CaCh 2a subtype of the cardiac α_1 subunit, prepared its RNA transcript, and expressed it in Xenopus laevis oocytes along with transcripts of the skeletal muscle β and γ subunits. In this report we describe the following three effects of the β subunit on the currents elicited from the α_1 subunit: 1) an increase in the peak current at all test potentials, 2) a shift in the threshold potential for activation, and 3) an acceleration of the kinetics of activation. The γ subunit had no significant effect on currents elicited by α_1 alone. In contrast, γ potentiated all three observed effects of β on α_1. These results indicate that the skeletal muscle β and γ subunits can interact, and thereby modulate the biophysical properties of the cardiac α_1 subunit. These results suggest that the cardiac L-type calcium channel may have a subunit structure that is similar to that of skeletal muscle.

6.2

POSSIBLE BRAIN CHANNELS: A COMPARISON OF PENETRATION AND RETENTION OF THE p-I-131-IODOBENZYLAMINO DERIVATIVES OF ADAMANTANE AND ISOBORANE. M.K. Karimeddini,*E.E. Leutzinger,* H.K. Patel,* R.P. Spencer. Dept. Nuclear Medicine. Univ. Connecticut Health Center, Farmington, CT 06030.

Adamantane has been utilized in the treatment of influenza and some neurological disorders. These actions may be due to membrane interactions and/or effects on channels to the central nervous system. To gain some understanding of this, we have expanded initial observations on the biodistribution of the p-I-131-iodobenzylamino derivatives of adamantane (I-ADA) and of the related compound isobornylamine (I-ISO).

After synthesis of the unlabeled compounds and identification by NMR and elemental analysis, partition was studied in the system octanol/phosphate buffer as a function of pH. The synthesis was then repeated with radioiodide (I-131) to produce a high specific activity product.

Biological studies were carried out in Swiss CD-1 mice of both sexes and in white male rabbits. Intravenous administration was accomplished using variations on H2O/DMSO solutions. After sacrifice, blood and organs were weighed, counted for radioactivity and compared with standards. The I-ADA had entered the brain and showed persistence.By contrast, the closely related I-ISO had little penetrance or persistence in the brain, despite fairly similar partition characteristics. Synthesis & testing of additional analogues may be of use in defining characteristics for channel penetration to the CNS.

6.3

THE GATING MECHANISM OF K CHANNELS AS REVEALED BY PORE STRUCTURE. Chyuan-Yih Lee. Advantage Capital Corp., 204 Executive Drive, Guilderland, NY 12084.

Experiments (Science, 251, 939-942, 1991) have demonstrated that SS1-SS2 could be the pore-forming region. If the side-chains of tyrosines at position 445 of four subunits are pointing toward the pore, they can make hydrogen bonds with each other, forming the closed state of the channel. Tyrosine is known to be involved in many electron transfer reactions. As the electron leaves its phenol OH group, the OH bond is broken. The deprotonated tyrosines become tyrosine radicals. Since there is no hydrogen bonding between tyrosine radicals, they may bend toward the extracellular or intracellular side, making more room for the ions to pass through. The O atoms of the tyrosine radicals can also facilitate the permeation of ions. The electron from tyrosine 445 may jump to tryptophan 434 or 435 since, among all amino acid residues, tryptophan is the most likely electron acceptor from tyrosine. Aspartate 447 could be the voltage sensor. Upon depolarization, the negative charge of aspartate 447 may be pulled toward tyrosine 445, increasing the electron transfer probability. When the negative charge of aspartate 447 is neutralized by proton, electron transfer from tyrosine 445 would be less likely and the channel may be closed despite depolarization. This agrees with the observation that the channel may be blocked by protons from extracellular side.

6.4

ION SELECTIVITY PROFILES OF AMPHOTERICIN B CHANNELS IN LIPID VESICLES. Scott C. Hartsel, Sandra K. Benz, Woubeshet Ayenew and Thomas Stephan. University of Wisconsin-Eau Claire, Eau Claire WI 54702.

Amphotericin B (AmB) is an antifungal polyene antibiotic and model ion channel which presumably acts via membrane association of monomers. We have measured the monovalent cation selectivity sequence of Amphotericin B structures in both small and large lipid membrane vesicles (SUV and LUV) using the pH sensitive probe pyranine. We have also studied divalent cation permeability and selectivity properties. In these experiments H^+ was exchanged for the transported cation by making the membrane highly permeable to protons with the protonophore FCCP. A stopped-flow system was used to introduce the antibiotic and/or create a salt gradient. When different cationic species were present on either side of the membrane, a bi-ionic potential developed. The direction and magnitude of the resulting pH change indicated which, if any, cation was more permeant in the AmB channel. The sequence determined for sterol-free SUV and cholesterol containing SUV and LUV, $Na^+ > K^+ > Rb^+ > Cs^+ > Li^+$ (sulfate salts), corresponds closely to Eisenman selectivity sequence number VII. This is the only case of which we are aware that a small model channel forming compound has shown $Na^+ > K^+$ selectivity, *including Na^+ channel peptides*. This sequence deviates from the sequence previously determined for AmB channels in cholesterol-containing planar bilayers. AmB channels in sterol-free vesicles were impermeant to Ca^{2+} ions when $CaCl_2$ gradients were imposed. This indicates that sterol-free channels may pass monovalent but not divalent cations. In contrast, in AmB treated vesicles containing 10 mole percent cholesterol, a modest Ca^{2+} permeability enhancement was observed and vesicles with ergosterol (the normal fungal sterol) a much higher Ca^{2+} permeability was seen. Ca^{2+} permeability has also not been reported in BLM studies. These differences in selectivity indicate that Amphotericin B channels can adopt a multiplicity of structures depending upon the local membrane environment. The difference between ergosterol and cholesterol channel selectivity may have great importance concerning the mechanism of selective toxicity of AmB toward fungal cells and on the nature of AmB channels.

6.5

A NOVEL PHYSICAL MODEL FOR VOLTAGE-DEPENDENT GATING OF L-TYPE CALCIUM CHANNELS. Craig A. Doupnik and R.Y.K. Pun, Dept. Physiol. & Biophys., Univ. of Cincinnati, Cincinnati, OH 45267.

We examined the effects of phosphorylation on voltage-dependent gating of L-type Ca^{2+} channels in bovine adrenal chromaffin cells under whole-cell voltage clamp. 8-bromo cAMP (1 mM) or phorbol ester (80 nM TPA) increased evoked Ca^{2+} and Ba^{2+} currents, and shortened the activation time in a voltage-dependent manner. Steady-state voltage-dependent activation curves under phosphorylating conditions were significantly shifted 6-10 mV more negative. The steepness of the relations were also increased and corresponded to an increase of ~1 charge in the activation gate valency (z_m). Channel gating rates derived according to a m^2 Hodgkin-Huxley activation process indicated that the forward rate (α_m) for channel activation was increased at membrane potentials $\geq$ 0 mV, and the backward rate (β_m) decreased at potentials $\leq$ 0 mV. Such results are not predicted by the "helical screw" model for voltage-dependent gating and the putative molecular structures of L-type Ca^{2+} channels. Our results can be explained by a more holistic model where the voltage sensor is represented as a dipole that arises from fixed charges within the tertiary structure of the channel protein. To account for our data, the dipole must be oriented in a less stable conformation at hyperpolarized resting potentials, where upon depolarization, it readily aligns itself with the electric field and confers channel opening. In this configuration, an increase in the dipole moment by phosphorylation would cause enhanced voltage sensitivity and the altered gating transition kinetics observed. Supported by NSF grant DCB8812562.

6.6

CALCIUM PERMEATION OF VOLTAGE-DEPENDENT SODIUM CHANNELS AT LARGE DRIVING FORCES. Beth B. Hogans and Bruce K. Krueger. Department of Physiology, University of Maryland School of Medicine, Baltimore, Maryland 21201.

We have studied divalent cation block of sodium channels over an extended voltage range from -160 to +180 mV. Saxitoxin-sensitive, rat brain sodium channels were incorporated into planar lipid bilayers in symmetrical 500 mM NaCl and in the presence of both batrachotoxin and scorpion (*L. quinquestriatus quinquestriatus*) venom. In the absence of divalent cations the single channel current-voltage (i-V) relationship was linear with a conductance of about 28 pS. Addition of 15 mM Mg^{2+} or Sr^{2+} to the extracellular side caused voltage-dependent block: fractional block increased monotonically as the membrane was hyperpolarized from -70 to -160 mV. In con-trast, block by 15 mM external Ca^{2+} was relieved at potentials more negative than -130 mV. From -140 to -160 mV, the single channel conductance was >20 pS. A 3-barrier 2-site Eyring rate theory model with binding sites at δ's of .36 and .93 fit the data using central barrier heights of 22.2, 16.5 and 9.0 RT units for Sr^{2+}, Mg^{2+} and Ca^{2+}, respectively. Data from the block of Na^+ current by internal Ca^{2+} was used to determine the position of the internal site. These results show that the open sodium channel is significantly permeable to Ca^{2+}, but that large hyperpolarizing potentials are necessary to drive Ca^{2+} inward through the channel. Supported by NIH grant NS16285 and a Howard Hughes predoctoral fellowship.

6.7

A REEXAMINATION OF THE MECHANISM OF BLOCKADE OF THE DELAYED RECTIFIER (I_K) BY TEA$^+$. MUST THE CHANNEL OPEN FOR BLOCKADE TO OCCUR? John R. Clay.
NIH, Bethesda, MD 20892

Blockade of I_K by tetraethylammonium ions (TEA^+) is believed to occur after the I_K channel has been opened by membrane depolarization. However, the original evidence for this view is consistent with an alternative scheme in which blockade can occur equally well when the channel is either open or closed. Tail current kinetics distinguish between these two models. The tail current time constant (τ_t) is unaltered if blockade is independent of channel state, whereas τ_t is increased if blockade occurs only in the open state because the blocker must leave the channel before the gates can close. Tail current measurements from I_K in squid axons are consistent with the independence scheme for $TEA^+(C_2)$ and C_3. Longer chain triethylammonium ion derivatives (C_n, n >3) increase τ_t in a manner which is consistent with the traditional view of TEA^+ blockade. These results demonstrate that seemingly minor changes in the structure of a blocking ion can significantly alter the mechanism of blockade.

6.8

A DETAILED STRUCTURAL MODEL OF THE TRANSMEMBRANE PORTION OF VOLTAGE-GATED POTASSIUM CHANNELS.
H. Robert Guy and Stewart R. Durell, Lab. Math. Biol., NCI, NIH, Bethesda, MD 20892.

Experiments in several laboratories have supported our postulates that each of four homologous domains of sodium and calcium channels or each of four identical subunits of potassium channels have eight transmembrane segments (S1, S2, S3, S4, S5, SS1, SS2, and S6), and that negatively charged SS1 and SS2 segments form the ion selective pore. We are now using computer graphics and molecular mechanics calculations to develop models that specify positions of all atoms in the transmembrane region. We have developed a series of models that have the following properties in common. The SS1 and SS2 segments form an eight-stranded antiparallel ß-barrel. The length of this barrel and the residues that comprise it differ among the models. The ß-barrel is surrounded by S6 helices and by S4 helices and the L45 helices linking S4 to S5. The S4 helices are near the external surface and are almost parallel to the plane of the membrane (as are the N-terminal helices of S6) when the channel is open. An outer cylinder comprised of S1, S2, S3, and S5 α-helices spans the entire membrane. The intracellular entrance of the channel is large when the channel is open because the ß-barrel does not span the entire membrane. Highly conserved residues tend to pack next to other highly conserved residues and nonfunctional surface residues tend to be poorly conserved. A conserved disulfide bond links the S6 helix to the S2 helix. We are examining possible activation gating and TEA binding mechanisms.

6.9

EXPRESSED Na CHANNEL CLONES DIFFER IN THEIR SENSITIVITY TO EXTERNAL [Ca]. M. Chahine, L. Chen*, R. Kallen*, R. Barchi* and R. Horn. Dept. of Neurosciences, Roche Inst. of Molec. Biol., Nutley, NJ 07110. *Dept. of Biochem. & Bioph. and Med. & Mahoney Inst. for Neurological Sci., Univ. of Pennsylvania, Philadelphia, PA 19104. SPON: J. Reeves

Two types of sodium channels, tetrodotoxin (TTX) sensitive Na channel (Kd=1nM) and TTX resistant (Kd=1µM) coexist in developing and denervated rat skeletal muscle. The sensitivity of these channels to TTX has been examined extensively using binding and patch-clamp studies. SkM1 (TTX sensitive) and SkM2 (TTX resistant) Na channels, cloned from rat denervated skeletal muscle and expressed in Xenopus oocytes after mRNA injection, show different sensitivity to extracellular calcium. The effect of [Ca] on SkM1 and SkM2 was investigated using outside-out patches from oocytes. Single channel analysis shows different conductances of SkM1 (32 pS) and SkM2 (10 pS) in normal saline containing 1.5 mM Ca. The slope conductance of SkM1 is higher than reported for TTX sensitive Na channels of developing rat skeletal muscle (R. Weiss and R. Horn, 1986). Changing the [Ca] from 1.5 mM to 10 mM induced a fast block of open channels as seen by a decrease in the amplitude of unitary currents of SkM1. This effect was greater at more hyperpolarized voltages. At 0 mM Ca, the conductance of the Na channels was found to be higher (42 pS). The voltage dependence of the Ca block of SkM1 channels is consistent with a binding site within the pore. In contrast the conductance of SkM2 was only slightly changed by external [Ca]. The difference between SkM1 and SkM2 can be explained by a different affinity of Ca for a blocking site in the open channel.

6.10

Characterization of Calcium Entry and a Novel Calcium Channel Cloned from Murine Erythroleukemia Cells
Boaz Gillo, Yong-Sheng Ma, Qing Liu, Ding-Ming Yang and Andrew R. Marks. SPON: Peter Harpel Mount Sinai School of Medicine, New York, N.Y.

Murine erythroleukemia cells (MELC) are an excellent model for examining cell growth and differentiation. Hexamethylene bisacetamide (HMBA) induces MELC to commit to terminal differentiation. In fluo-3 loaded MELC, HMBA induces a 40% to 400% increase in fluorescence within 2 to 8 minutes which depends on $[Ca^{2+}]_{out}$. Moreover, EGTA added to the culture media (reducing $[Ca^{2+}]_{out}$ to <2µM) blocks HMBA induced differentiation in MELC. Based on these and other observations we have used cDNA probes from the dihydropyridine receptor (DHPR) to isolate cDNA encoding a novel calcium channel from MELC. This novel calcium channel (MELC-CC) is highly homologous to the cardiac DHPR but lacks the putative IIIS1 transmembrane segment and has other deletions, insertions, and additions. Culturing MELC with MELC-CC antisense oligonucleotides reduced HMBA induced commitment to differentiation by 50%. The novel MELC calcium channel may play a role in calcium entry required for cell differentiation.

6.11

A ß-BARREL MODEL FOR THE PORE OF THE VOLTAGE-GATED POTASSIUM CHANNEL. S. Bogusz[1], A. Boxer[1], J.A. Drewe[2], G.E. Kirsch[2], H. Hartmann[2], M. Taglialatela[2], A. M. Brown[2], R. Joho[2], and D. Busath[1]. [1]Section of Physiology, Box G-B302, Brown University, Providence, RI 02912 and [2]Dept. of Molec. Physiol. and Biophys., Baylor College of Medicine, Houston, TX 77030.

To examine the feasibility of a ß-structure for the pore-lining region of the voltage-gated potassium channel (Yellen, et al., Science 251:939, 1991; Yool and Schwarz, Nature 349:700, 1991; Hartmann, et al., Science 251:942, 1991), we have constructed a ß-barrel using molecular mechanics. Each of four DRK/NGK monomers contribute a pair of ß-strands from the S5-S6 linker (residues 362-369 and 373-380) to form an eight-stranded anti-parallel barrel. The barrel is organized so that side chains that strongly affect external TEA block, internal TEA block, and ionic selectivity project into the barrel. These constraints require that the hairpin turn between the strands consist of an odd number of amino acids including M371 (=Shaker:M440) and suggest that the strands be organized so that the S6 end is counterclockwise from the S5 end in the extracellular view. Following precedents from other proteins of known structure and potential energy predictions, the barrel is right-tilted. Energy minimization yielded a structure with favorable potential energy. The interior of the channel is densely packed with side chains, but on the whole, the structure has favorable van der Waals interactions.

6.12

MUTATIONS IN THE LEUCINE HEPTAD REPEAT OF *SHAKER* 29-4 ALTER THE CHANNEL'S ACTIVATION WITHOUT ALTERING GATING CURRENTS
Nathan E. Schoppa,* Ken McCormack,* Mark A. Tanouye,# and Fred J. Sigworth,* *Dept. of Cellular and Molecular Physiology, Yale University School of Medicine, New Haven, CT 06510, #Dept. of Entomology, University of California, Berkeley, CA 94720.

Mutating either of the first two leucines in the conserved heptad repeat region of *Shaker* cDNA 29-4 to valines causes a 60-100 mV depolarizing shift and a dramatic reduction in the voltage sensitivity of channel activation (McCormack et al., PNAS 88: 2931). In search of an explanation for these changes, we recorded "macroscopic" ionic currents and gating currents in membrane patches from oocytes injected with mRNA encoding non-inactivating wild-type and mutant channels. All recordings were made in the inside-out mode with an N-Methyl-D-Glucamine Aspartate pipette solution. Bath solutions contained K-Asp and Tetraethylammonium (TEA) Asp for measuring ionic and gating currents, respectively. Gating current measurements showed that the voltage dependence and kinetics of most of the charge movement were similar in the wild-type and mutant channels. Moreover, the number of effective charges displaced per channel opening appeared to be similar for the two channels. Lower bounds for z obtained from the limiting slopes of the activation curves (at P(o) < 0.01) were similar : 9.9±1.3 (N=4) and 8.7 (N=2) for wild-type and mutant channels. These values were close to those obtained from experiments which directly evaluated z. First, the number of channels in a patch was estimated from noise analysis on ionic currents; then, following the replacement of K with TEA, the charge movement was measured in the same patch. From these measurements, z was calculated to be 9.7±0.5 (N=4) and 8.8±2.6 (N=3) for the wild-type and mutant channels. The mutation appears to affect steps in the activation process that follow most of the charge displacement.

6.13

ISOLATION AND BIOCHEMICAL CHARACTERIZATION OF THE RABBIT BRAIN ω-CONOTOXIN GVIA RECEPTOR. Junshi Sakamoto and Kevin P. Campbell. Howard Hughes Medical Institute and Department of Physiology and Biophysics, University of Iowa College of Medicine, Iowa City, Iowa 52242.

Neuronal voltage-gated Ca^{2+} channels exist in several subtypes (L, N, T and P) which have different kinetic and pharmacological properties. L-type channels are sensitive to dihydropyridines. N-type channels are inhibited by ω-conotoxin GVIA (ω-CgTX) and may be responsible for the Ca^{2+} influx which triggers neurotransmitter release at synapses. Although several antibodies are reported to react with the brain dihydropyridine receptor, no antibodies specific for the ω-CgTX receptor have been reported. In addition, neuronal Ca^{2+} channels have not been purified and their molecular structures and subunit compositions are still unknown. We have found that monoclonal antibody (mAb) $VD2_1$ against the β subunit of the skeletal muscle Ca^{2+} channel specifically immunoprecipitates up to 86% of the ω-CgTX receptor solubilized with digitonin. The immunoprecipitated receptor showed high affinity $[^{125}I]$ω-CgTX binding, which was inhibited by unlabeled ω-CgTX and by $CaCl_2$, but not by nitrendipine or by diltiazem. We now report the isolation of the ω-CgTX receptor using affinity chromatography with mAb $VD2_1$. Rabbit brain membranes were preincubated with $[^{125}I]$ω-CgTX, solubilized with digitonin, and first applied to a heparin-agarose column. The eluate of the heparin-agarose was then applied on a column of mAb $VD2_1$-Sepharose and the receptor was eluted with an alkaline buffer. $[^{125}I]$ω-CgTX remained bound to the receptor, suggesting that the receptor maintained its active conformation. The alkaline eluate from the affinity column contained several proteins including 78-kDa and 58-kDa proteins, which bound mAb $VD2_1$ and other anti-β subunit antibodies. Preliminary results of sucrose density gradient centrifugation suggest that the subunit composition of the brain ω-CgTX receptor is similar to, but distinct from that of the skeletal muscle Ca^{2+} channel.

RECEPTOR-EFFECTOR SIGNALLING AND E-C COUPLING

7.1

AVIAN EXTENDED JSR (EJSR): A CHALLENGE TO DIRECT CONTACT SIGNAL TRANSDUCTION (DCT) FOR COUPLING EXCITATION TO CALCIUM-RELEASE (ECR) IN CARDIAC MUSCLE. Joachim R. Sommer, Edward Bossen, Rashid Nassar. Depts. of Pathology and Cell Biology, Duke Univ. Medical Center, and VA Hospital, Durham, NC, 27710

JSR stores calcium for ECR. JSR is intercalated into a network of free SR, usually at Z lines, and contains electron-dense, highly negatively charged material that often also occurs in spots in the free SR outside the JSR (perhaps constituting the elusive "calciosomes"?). In skeletal muscle, the junctional membrane proper of the JSR is covered by junctional processes (JP) that harbor Ca-release channels and face the plasma membrane (PM). In cardiac muscle, however, the JPs, in addition, are frequently facing, and end freely in, the cytoplasm. JSR forms so-called "couplings" with the plasma membrane (PM) across a narrow cytoplasmic junctional gap of rather constant width. In avian hearts, in which transverse tubules are absent, 80% of the total JSR is separated by several microns from the PM, by which topographical feature JSR becomes EJSR by definition (except for PM attachment, EJSR and JSR are anatomically identical); but, significantly, only 20% of the total JSR remains part of "couplings" (i.e. as JSR proper) whereas, in mammalian hearts (excepting the rare corbular SR), almost 100% of JSR is part of "couplings". By stereologic quantitation, and given similar heart rates and sizes, the total JSR volume fractions in myocytes of mice (JSR) and finches (JSR + EJSR) as well as their surface to volume ratios are virtually identical. **Conclusion:** 1) The topography of EJSR proscribes DCT and favors a diffusible transmitter substance for ECR. 2) Since quantitative comparative anatomy suggests anatomical and functional homology of EJSR and JSR, the topography of EJSR points to the JSR of "couplings" in cardiac (and skeletal?) muscle as serving an additional function that depends uniquely on PM-attachment (intermittent opening to the extracellular space, perhaps by specialized JPs, may be such a function). (Support: NIH HL12486 and the VA Research Service)

7.2

ROLE OF PARVALBUMIN (PA) IN FROG SKELETAL MUSCLE RELAXATION. J.A. Rall, T.-t. Hou & J.D. Johnson. Ohio State University, Columbus, OH 43210.

PA is an intracellular Ca^{2+}-binding protein which may promote relaxation in fast contracting skeletal muscle. If PA promotes relaxation, its effect would diminish with increasing tetanus duration since PA binds Ca^{2+} during contraction. Time course of slowing of relaxation rate should be limited by Mg^{2+} dissociation from PA since PA contains Mg^{2+} at rest. At 0 °C relaxation rate slows exponentially ($1.18\ s^{-1}$) with increasing tetanus duration in fibers isolated from tibialis anterior muscles of the frog, *R. temporaria*. If PA promotes relaxation, recovery of relaxation rate after a prolonged tetanus should be limited by Ca^{2+} dissociation from PA. Recovery of relaxation rate is exponential ($0.12\ s^{-1}$). To test these predictions for dissociation of Mg^{2+} and Ca^{2+} from PA, off rates were determined with purified PA (IV_b) by stopped-flow techniques using terbium as a reporter group. Mg^{2+} ($0.93\ s^{-1}$) and Ca^{2+} ($0.19\ s^{-1}$) off rates are similar to rates predicted from physiological results. Similar relationships were observed at 10 °C. Thus evidence supports a role for PA in promoting relaxation in frog skeletal muscle. Supported by NIH AR20792.

7.3

INHIBITORY MECHANISMS OF K CHANNEL OPENERS ON AGONIST-INDUCED CONTRACTIONS IN CORONARY ARTERY. Teruyuki Yanagisawa and Norio Taira. Dept. Pharmacol., Tohoku Univ. Sch. Med., Sendai 980, Japan.

It is well-known that the contractions induced by agonists in vascular smooth muscle are inhibited well by K channel openers. To clarify the inhibitory mechanisms, we examined how the changes in membrane potentials affect the contraction induced by a thromboxane A_2 analogue, U46619 (U), by simultaneously measuring $[Ca^{2+}]_i$ and the force of contraction in canine coronary arteries. The U-induced increases in $[Ca^{2+}]_i$ *via* both release from the store and the influx and related contraction were inhibited by cromakalim, and the increase in $[Ca^{2+}]_i$ *via* influx was potentiated by the depolarization by 20 mM KCl. When the hyperpolarization by cromakalim was counteracted by 20 mM KCl or blocked by a K channel blocker, tetrabutylammonium, U produced the same increases in $[Ca^{2+}]_i$ and contraction as in control. Thus, the inhibitory effects of K channel openers are due to the 'deactivation' of L-type Ca channels and the inhibition of Ca^{2+} release from the store by hyperpolarization of plasma membrane.

7.4

REGULATION OF CONTRACTILE PROPERTIES BY MUSCARINIC RECEPTOR STIMULATION IN FERRET VENTRICULAR MUSCLE S. Kurihara, K. Hongo and E. Tanaka. Dept. of Physiol., The Jikei Univ. School of Med., Tokyo 105 Japan

We investigated the mechanism of muscarinic receptor stimulation which alters the time course of twitch tension in ferret ventricular muscle. Aequorin was used to monitor the intracellular Ca transients (CaT), and a perturbation analysis method was employed to measure the cross bridge cycling rate (CCR). Addition of acetylcholine (ACh) or carbachol to the preparation treated with isoproterenol (Iso) recovered the time course of CaT and the time to peak tension. But the half relaxation time was further shortened by ACh. The Ca sensitivity of the contractile element (CaS) which was decreased by Iso was recovered by ACh. The Iso-accelerated CCR was also recovered by ACh and the effect of ACh was blocked by atropine. The effects of ACh were not observed in preparations from ferrets treated with pertussis toxin. These results suggest that the primary effect of muscarinic receptor stimulation is inhibition of adenylate cyclase through Gi and that factors other than CaT, CaS and CCR are involved in the determination of the relaxation time.

7.5

THE Ca^{++}-SENSITIVITY OF THE PHOTOPROTEIN HALISTAURIN IS NOT INFLUENCED BY PHYSIOLOGICAL CONCENTRATIONS OF Mg^{++}. John R. Blinks and Dorothy D. Caplow*. Friday Harbor Laboratories, University of Washington, Friday Harbor, WA 98250.

One of the disadvantages of the Ca^{++}-regulated photoprotein aequorin as an intracellular Ca^{++} indicator is that its Ca^{++} sensitivity and kinetics are influenced by the concentrations of Mg^{++} found in the cytoplasm of living cells. We have found that Mg^{++} has very much less effect on the closely related photoprotein halistaurin.

Halistaurin was isolated from the luminescent jellyfish Halistaura (Mitrocoma) cellularia, and purified by gel filtration and ion-exchange chromatography (two stages each). Full Ca^{++}-concentration-effect curves were determined in solutions containing 150 mM K^+ and various [Mg^{++}] (20°C., pH 7.0). The curve for halistaurin is similar in amplitude and shape to that for aequorin, and lies between the aequorin curves determined in 0 mM and 1 mm Mg^{++}. Concentrations of Mg^{++} up to 1 mM had no influence on either the level of the calcium-independent luminescence (CIL) or the Ca^{++}-sensitivity of halistaurin; 3 mM Mg^{++} increased the CIL slightly, but did not have an appreciable effect on the response to Ca^{++}. Support: HL 12186.

7.6

INTERACTIONS OF THE α SUBUNITS OF THE SKELETAL MUSCLE DIHYDROPYRIDINE RECEPTOR. Bernhard E. Flucher, Johanna L. Phillips and Jeanne A. Powell. Lab. of Neurobiology, NINDS, NIH, Bethesda, MD and Dept. of Biological Sciences, Smith College, Northampton, MA.

We have studied the subcellular distribution of the α_1 and α_2 subunits of the skeletal muscle dihydropyridine (DHP) receptor with immunofluorescence labeling of normal and dysgenic (*mdg*) mouse muscle in culture. In normal myotubes both α subunits were localized in clusters associated with the T-tubules. During development the DHP receptor-rich domains became organized periodically in the sarcomeres prior to the transverse organization of the T-tubules. In well developed myotubes the DHP receptor (α_1 and α_2) clusters were lined up in rows on both sides of the Z-line similar to the labeling pattern observed in mature muscle. Thus the DHP receptor-rich domains may represent the sites of triad formation. In cultures from dysgenic muscle the α_1 subunit was undetectable and the distribution patterns of the α_2 subunit were abnormal. The α_2 subunit did not form clusters nor was it discretely localized in the T-tubule system. Instead, α_2 was found diffusely distributed in parts of the T-system, in structures in the perinuclear region and in the plasma membrane. These results suggest that an interaction between the two α subunits is required for the normal distribution of the α_2 subunit in the T-tubule membranes. In heterokaryons of dysgenic muscle and normal non-muscle cells from rat, expression of the α_1 subunit was restored in the vicinity of the normal nuclei and several adjacent dysgenic nuclei. In these regions the α_1 subunit appeared in its normal clustered distribution. Furthermore, the normal intracellular distribution of the α_2 subunit was restored in domains containing a foreign "rescue" nucleus; this supports the idea that direct interactions between the DHP receptor α_1 and α_2 subunits are involved in the organization of the junctional T-tubule membranes. (Supported by MDA & Smith Blakeslee Fund to J.A.P.)

7.7

PHOSPHOINOSITIDE HYDROLYSIS AND POSITIVE INOTROPIC EFFECT INDUCED BY ENDOTHELIN IN THE RABBIT VENTRICULAR MUSCLE. Masao Endoh and Masahiro Takanashi. Department of Pharmacology, Yamagata University School of Medicine, 990-23 Yamagata, Japan

Endothelin-1 (ET-1) elicited a concentration-dependent accumulation of [^{3}H]IP_1 in the rabbit ventricular slices prelabeled with [^{3}H]myo-inositol in the same concentration range that it caused a positive inotropic effect on isolated rabbit papillary muscle. The EC_{50} values for increase in both parameters were consistent and 6 nM. The accumulation of [^{3}H]IP_3 preceded to the positive inotropic effect of ET-1. The K_d value for specific binding of [^{125}I]-ET-1 to the membrane fraction derived from the rabbit ventricular muscle was 0.36 nM. A phorbol ester, phorbol 12,13-dibutyrate (PDBU, 10-300 nM) inhibited the positive inotropic effect and the accumulation of [^{3}H]IP_1 induced by ET-1 in a concentration-dependent manner. The positive inotropic effect of Bay k 8644 and isoproterenol was scarcely affected by PDBu at the concentration that it inhibited the ET-1-induced inotropic effect and [^{3}H]IP_1 accumulation. The specific binding of [^{125}I]-ET-1 to the membrane fraction was not affected by PDBu up to 1 μM. These findings strongly suggest the involvement of phosphoinositide hydrolysis in the positive inotropic effect of ET-1 in the rabbit ventricular muscle.

7.8

SELECTIVE INHIBITION BY STAUROSPORINE AND PHORBOL ESTER OF THE POSITIVE INOTROPIC EFFECT MEDIATED BY α-1 ADRENERGIC RECEPTORS. Masao Endoh, Masahiro Takanashi and Ikuo Norota. Department of Pharmacology, Yamagata University School of Medicine, 990-23 Yamagata, Japan

The positive inotropic effect of phenylephrine (PE, 10 μM) mediated by α-1 adrenergic receptors in the presence of bupranolol (0.3 μM) was inhibited by a selective protein kinase C (PKC) inhibitor staurosporine (STSP, 1-100 nM) in the rabbit papillary muscle. The effect of PE (0.1 mM) mediated by β receptors in the presence of prazosin (0.3 μM) was decreased first by 100 nM STSP. Newly developed PKC inhibitor NA 0345 (a derivative of SF 2370) caused likewise the preferential inhibition of the α-1 to β receptor-mediated effect. A PKC activator phorbol 12,13-dibutyrate (PDBu, 10-300 nM) also antagonized selectively the α-1-mediated inotropic effect in a concentration-dependent manner, while β-mediated effect being not inhibited. Phosphoinositide (PI) hydrolysis induced by α-1 stimulation detected as [^{3}H]IP_1 accumulation in the rabbit ventricular slices prelabeled with [^{3}H]myo-inositol was inhibited by PDBu (10-100 nM), while neither STSP nor NA 0345 affected the α-1-mediated [^{3}H]IP_1 accumulation. These findings support the physiological relevance of PI hydrolysis and activation of PKC for the positive inotropic effect mediated by myocardial α-1 receptors.

7.9

CHOLESTEROL MODULATES THE MEMBRANE BINDING OF 1,4-DIHYDROPYRIDINE Ca^{+2} CHANNEL BLOCKERS. R. Preston Mason and Lydia Shajenko. Biomol. Struct. Anal. Center. U. of Connecticut Health Center, Farmington, CT. 06032

The effect of cholesterol content on the membrane interactions of 1,4-dihydropyridine (DHP) Ca^{+2} channel blockers was examined using small angle x-ray diffraction and radioligand binding assays. Increases in membrane cholesterol content resulted in a dramatic decrease in the DHP membrane partition coefficients ($K_{P[mem]}$) and rates of membrane dissociation. These effects of cholesterol on membrane binding were more pronounced for the neutral DHPs isradipine and nimodipine than for the charged DHP, amlodipine. For example, $K_{P[mem]}$s for nimodipine and amlodipine were reduced 11 and 3 fold, respectively, between 0 and 37.5 mol% cholesterol in cardiac lipid extracts. Electron density profiles generated from the x-ray diffraction data showed that the membrane time-averaged location for the DHP and cholesterol molecules overlap, suggesting that the addition of cholesterol decreases the available volume for DHP partitioning in the membrane. These data may help to explain the distinct pharmacological properties of the DHPs, especially under conditions of atherosclerosis in which smooth muscle plasma membrane cholesterol content has been shown to increase by 80% [FASEB 5:531a (1991)]. (Supported by AHA, CT Affiliate; John Hartford Foundation and Pfizer Labs.)

7.10

CALCIUM-INDUCED CALCIUM RELEASE IN CRAYFISH MUSCLE FIBERS. **Sandor Gyorke and Philip Palade, SPON: Luis Reuss. Dept. Physiology and Biophysics, Univ. Texas Medical Branch, Galveston, TX 77550**

I_{Ca} and intracellular Ca^{2+} transients (Δ[Ca]) were recorded in cut crayfish muscle fibers using the fluorescent Ca^{2+} indicator Rhod-2 and the Vaseline-gap voltage-clamp technique. Ca^{2+} transients depended on the amplitude of I_{Ca} and were 90 % inhibited by the SR Ca^{2+} release blocker procaine (10 mM), which only decreased I_{Ca} by 10 %. I_{Ca} inactivation was slightly slowed by procaine, while 0.5 mM caffeine had the opposite effects on I_{Ca} and Δ[Ca]. 15 % of fibers showed a continued climb in Δ[Ca] after termination of short pulses, but amplitude remained graded by I_{Ca}. These results can be explained in terms of a model where Ca^{2+} binding sites for inactivation of I_{Ca} (X) and for activation of SR calcium release (Y) are located in a restricted space remote from the cytoplasmic mouth of the SR Ca^{2+} release channel. This interpretation has important ramifications for E-C coupling in both cardiac and vertebrate skeletal muscle.

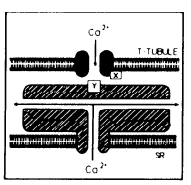

7.11

^{125}I-CALMODULIN BINDING TO PROTEINS IN SARCOLEMMAL MEMBRANE FRACTIONS FROM MAMMALIAN HEART. Donald D. Doyle and Yuee Guo. The University of Chicago, Chicago, Illinois 60637

Surface and t-tubular membrane fractions from adult sheep heart, enriched 50-fold over homogenate values in myocyte—specific low affinity binding of ^{3}H-saxitoxin to heart-type sodium channels (Doyle and Winter, J. Biol. Chem. **264**:3811, 1989) — were analyzed for the presence of proteins which bind calmodulin (CaM). ^{125}I-CaM binding at 20 nM concentration was detected on nitrocellulose overlays of membrane proteins fractionated by SDS-PAGE. The most strongly labeled bands, a doublet at 130-150 kilodaltons (kD), were enriched in our sarcolemmal (SL) preparation relative to a preparation of sarcoplasmic reticulum membranes analyzed in parallel. We are currently testing whether one of these bands might be the putative SL Ca-ATPase. In addition, other CaM staining bands were seen at 220, 175, 85, 80, 55, 50, and 40 kD. The cytosolic fraction contained a band which comigrated with that seen at 50 kD in the SL fraction and which previous results suggest is Ca/CaM kinase type II (Doyle, *et al.*, J. Biol. Chem. **261**:6556, 1986). When the membranes were dissolved with 4 volumes of 0.5% Triton X-100 and separated by centrifugation at 100,000 × g into a Triton-soluble supernatant (presumed membrane protein) and a Triton-insoluble pellet (presumed cytoskeletal protein), bands at 40-100 and 220 kD appeared in the pellet, whereas bands from the range 100-200 kD remained primarily in the supernatant. We will attempt to characterize these proteins by correspondence with known CaM-binding proteins. Supported by USPHS grant HL 44004.

7.12

SMOOTH MUSCLE $[Ca^{2+}]_c$ IN RESPONSE TO Ca^{2+} INFLUX THROUGH VOLTAGE AND RECEPTOR OPERATED CHANNELS. G.Isenberg, P.Schneider, V.Ya.Ganitkevich. Dept. Physiology, University of Cologne, 5000 Köln 41, Germany. Sponsored by M. Morad.

In myocytes isolated from the urinary bladder of the guinea-pig, 100 μM Na_5-Indo1 was loaded through the patch pipette. At a holding potential of -60 mV, resting $[Ca^{2+}]_c$ was 114 ±22 nM (mean ±S.D.). 160 ms steps to 0 mV induced an I_{Ca} that incremented total intracellular Ca by approx. 50 μM (2 mM $[Ca^{2+}]_o$, 37°C). $[Ca^{2+}]_c$ rose along a time course proportional to the time integral of I_{Ca} to 885 ± 140 nM (peak at 0.6 s). However, it is unlikely that the fast rise and the peak are the direct result of Ca^{2+} influx; contribution of Ca^{2+} induced release of Ca^{2+} (CIRC) from the SR is suggested by the effects of caffeine (10 mM) or ryanodine (10 μM) which attenuated and delayed the peak.

P_{2x} purinoceptors were activated by bath application of ATP (50 μM). At -60 mV, it induced an inward current of approx. -1 nA which increased $[Ca^{2+}]_c$ to 730 ±100 nM at a maximal rate that was about 10% of the one measured during I_{Ca}. Pre-treatment of the cell with 20 mM caffeine or 5 mg/l intracellular heparin did not reduce the ATP-induced rise in $[Ca^{2+}]_c$ suggesting that it is mostly due to Ca^{2+} influx; because of its low rate, ATP-induced Ca^{2+} influx may have failed to induce CIRC. When depolarizations were induced on top of the ATP-induced $[Ca^{2+}]_c$ transients they failed in inducing I_{Ca} because of 'Ca^{2+} inactivation of I_{Ca}'. Thus, the effects were not additive.

7.13

INTRACELLULAR SODIUM GRADIENTS IN STIMULATED GUINEA-PIG VENTRICULAR MYOCYTES: AN X-RAY MICROPROBE STUDY. Maria Fiora Wendt-Gallitelli and Gerrit Isenberg. Dept. Physiology II, University of Tübingen and Dept. Physiology, University of Cologne, Köln, Germany. Sponsored by M. Morad.

At 36 °C, 2 mM $[Ca^{2+}]_o$ and 10 mM Na^+ in the patch pipette myocytes were voltage-clamped with paired pulses at 1 Hz; a first 160 ms pulse to 0 mV activated Ca^{2+} influx through L-type channels, the second pulse to 50 mV Ca^{2+} influx through the Na,Ca-exchanger. Repolarization to diastolic -80 mV induced a large negative tail current indicative Na^+ influx through the Na,Ca-exchanger. When contractions and tail currents had been potentiated to a maximum (≥8 paired pulses), shock-freezing was timed at the end of the 600 ms diastole and total [Na] was analyzed by X-ray microanalysis. In the central myofibrillar space $[Na]_c$ was 48 ±8 mmol/kg d.w. which can be translated into 12 ±2 mM. $[Na]_c$ was similar as the 10 mM in the patch pipette and did not significantly change during potentiation. Underneath the peripheral sarcolemma, $[Na]_{sm}$ was 20 mM when the cells were at rest and reversibly increased to 34 ±9 mM upon potentiation. For potentiated cells, radial [Na] gradients were evaluated by both series of point-analysis with static probe and quantitative elemental digital imaging of larger submembraneous regions. At the inner side of the sarcolemma (indicated by a high total [K] of 450 mmol/kg d.w.) total [Na] was 200 mmol/kg d.w. as if Na had bound to membrane constituents. $[Na]_{sm}$ fell steeply towards the centre of the cell, 150 nm away from the membrane it was ≈100 mmol/kg d.w..

7.14

Development of peripheral couplings and triads reflects increase in DHP binding in chicken hind limb muscles. Hiroaki Takekura and Clara Franzini-Armstrong. University of Pennsylvania.

Specific binding of dihydropyridines (DHP) during development of chicken hind limb muscle has two periods of increase, a smaller one at ~ 9 dd. of incubation, and a second, larger starting at ~ 16 dd (Schmid, et al., J. Biol. Chem., 259, 11366, 1984). We test the hypothesis that junctional tetrads of triads and peripheral couplings are the DHP receptors. T-tubules were visualized by the K3Fe(CN)6 "staining", triads by thin sectioning, and j. tetrads in peripheral couplings by freeze fracture. Differentiation of membrane systems occurs in three stages: at 7 dd incubation, peripheral couplings and some internal, calsequestrin containing SR are present. Patches of junctional tetrads are present in the surface membrane and increase in density with time. At ~ 16 dd, T tubules develope suddenly, while myofibrils increase in number, nuclei migrate to the periphery, and primary and secondary fibers separate. Triads form immediately, and rapidly increase in number in parallel with increase in T tubules. Transverse orientation of T tubules occurs later. Thus, the two stages of DHP binding coincide with development of peripheral coupling and of triads.

7.15

Na/Ca EXCHANGE STUDIES IN FROG PHASIC MUSCLE CELLS. H. Gonzalez-Serratos, E. Castillo, M. Rozycka and *H. Rasgado-Flores. Dept. of Biophysics, School of Medicine, Univ. of Maryland, Baltimore MD; *Dept. of Physiol. and Biophysics, UHS/The Chicago Medical School.

Ca extrusion in phasic skeletal muscle may take place via a Na/Ca exchanger which has been poorly described. To further characterize this mechanism in isolated frog muscle cells, activity of the exchanger was studied by assessing the effect of various transmembrane Na^+ gradients on contractility. A decrease in the extracellular Na^+ concentration ($[Na^+]_o$) increased twitch tensions (up to 50%) and time to peak (up to 4.1 msec) with no change in twitch duration. Images of Ca release showed that low $[Na^+]_o$ resulted in an increase of intracellular Ca release proportional to the decrease in $[Na^+]_o$. To assess the effect of $[Na^+]_o$ < 55 mM, we tested it on K-contractures. The tension-[K] relationship in low $[Na]_o$ was steeper with no change in mechanical threshold and the same maximal tension as in high $[Na^+]_o$. Un-interrupted contractures in low $[Na^+]_o$ were larger and more prolonged than the ones in high $[Na^+]_o$. To assess the SR Ca pool we compared twitch potentiations due to low caffeine concentration (< 2 mM) evoked in high $[Na^+]_o$ with the ones elicited in low $[Na^+]_o$. The slope of the twitch tension-caffeine concentration relationship was steeper in the low $[Na^+]_o$. The difference in the slopes reflects the extra Ca available in low $[Na^+]_o$. The Na/Ca exchange blocker 3'-4' dichlorobenzamil (1 μm) produced a reversible 65% increase in twitch tension. The above results suggest the presence of a Na/Ca exchanger in phasic skeletal muscle cells driven by the Na gradient which will extrude the excess of Ca leaking into the cell, thereby keeping $[Ca^{2+}]_i$ in a steady state and mediates an increase in $[Ca^{2+}]_i$ when $[Na^+]_o$ is reduced. Supported by NIH Grant NS1708 (H. G-S) and AHA-Chicago Affiliate (H. R-F).

7.16

CHARACTERIZATION OF A FROG SKELETAL MUSCLE CONTRACTION MODULATOR. Nuran M. Kumbaraci*, Stevens Institute of Technology, Hoboken, New Jersey 07030

Frog skeletal muscle bathing in 1mM caffeine Ringer solution undergoes sarcomeric oscillations. When the bathing solution is applied to a fresh muscle sarcomeric contractions are initiated with a relatively short latency, (Kumbaraci, N. M. & Nastuk, W. L., J. Physiol. 325, 195-211, 1982). A UV absorption peak at 245 nm develops in the bathing solution with time. A fraction is obtained after chromatographic separation which has the UV peak and which initiates sarcomeric oscillations. The bathing solution was studied to characterize the properties of the bioactive compound(s). It was found that the height of the UV peak is directly proportional to the weight of the skeletal muscle tissue and reaches a maximum in 2 hours. The accumulation of this substance occurs in the absence of caffeine and a UV peak is seen at 247-249 nm. Precipitation, solubilization, solvent extraction, dialysis, Lowry protein assay along with absorbance correlation studies indicated that it is polar, heat stable, and protein in nature. Electrophoresis showed that there are several proteins in the solution. After Amicon filtration the active fraction was found to have a MW less than 1000 and HPLC separation showed two separate peaks. These results suggest that a small peptide is released from skeletel muscle in vitro and initiates sarcomeric contractions. This peptide may modulate excitation-contraction coupling at the T-tubule terminal cistern junction in skeletal muscle.

This work was in part supported by a grant from the Howard Hughes Medical Institute.

7.17

DIHYDROPYRIDINE RECEPTORS (DHPR) ARE PRIMARILY FUNCTIONAL L-TYPE Ca CHANNELS, BUT ARE OUTNUMBERED BY RYANODINE RECEPTORS (RYR) IN RABBIT CARDIAC MYOCYTES.

DM Bers, WYW Lew*, LV Hryshko & VM Stiffel, Div. Biomed. Sci., Univ. of Calif., Riverside, 92521 and *Univ. of Calif., San Diego, 92161

We measured DHPR and RYR density in rabbit ventricular homogenates and isolated myocytes. The DHPR density in homogenate was 75 ± 4 fmol/mg (K_d = 1.7 ± 0.3 nM) and in myocytes was 147 ± 6 fmol/mg (K_d = 1.2 ± 0.2 nM). Assuming 120 mg protein/cm³ heart, 25% extracellular space and a surface/volume ratio of 0.6 μm^{-1}, the DHPR density estimated from ventricular homogenate is 12.8 DHPR/μm^2 (or ~15 DHPR/μm^2 for myocyte data). The number of functional L-type Ca channels (N) was measured in isolated myocytes using voltage clamp and the formula $N = I/(i \cdot p_o)$, where I = peak whole cell current, i = single channel current, and p_o = global open probability. We measured Na current through Ca channels (I_{Na}) to prevent Ca_i-induced inactivation. Under similar conditions (140 mM NaCl, 4 mM EGTA, pH 7.4 at 22°C, E_m=-20) peak I_{Na} was ~105 pA/pF (n = 7), i_{Na} was 2.0 pA and the overall p_o was 0.030 ± 0.006 in patches with only a single channel (n = 16). The calculated density of functional L-type Ca channels was 18 channels/μm^2, similar to the DHPR density. RYR are 3.3-4 times more numerous (B_{max} =303 ± 9 fmol/mg homogenate pn and 486 ± 10 fmol/mg myocyte pn, K_d = 17 and 14 nM). We conclude that in cardiac muscle (and probably in skeletal muscle) the density of DHPR is similar to that of L-type Ca channels. The high ratio of RYR:DHPR implies that 2/3 - 3/4 of the RYR in cardiac muscle cannot be stoichiometrically associated with DHPRs (unless 3-4 high affinity RYR are coupled to each DHPR).

7.18

A MEMBRANE MODEL FOR CYTOSOLIC CALCIUM OSCILLATIONS: A STUDY USING *XENOPUS* OOCYTES. M. Saleet Jafri, Pedro Pasik, Sandor Vajda, and Boaz Gillo. SPON:Patrick Eggena. Mount Sinai School of Medicine, New York, NY 10029

Cytosolic calcium oscillations occur in a wide variety of cells and are involved in different cellular functions. We describe these calcium oscillations by a minimal mathematical model based on the putative electrophysiological properties of the endoplasmic reticulum (ER) membrane. The salient features of our membrane model are calcium-dependent calcium channels and calcium pumps in the ER membrane, constant entry of calcium into the cytosol, and calcium dependent removal from the cytosol. Numerical integration of the model allows us to study the fluctuations in the cytosolic calcium concentration and the ER membrane potential. The model demonstrates the physiological features necessary for calcium oscillations and suggests that the level of calcium influx into the cytosol controls the frequency and amplitude of oscillations. The model is supported by experiments indirectly measuring cytosolic calcium by calcium induced chloride currents in *Xenopus* oocytes as well as cytosolic calcium oscillations observed in other preparations.

CARDIAC ELECTROPHYSIOLOGY

8.1

DRUG-INDUCED AFTERDEPOLARIZATIONS AND TRIGGERED ACTIVITY OCCUR IN A SELECT SUBPOPULATION OF CELLS (M CELLS) IN THE DEEP SUBEPICARDIUM OF THE CANINE VENTRICLE.

Serge Sicouri, and Charles Antzelevitch. Masonic Medical Research Laboratory, Utica NY 13501.

We recently presented evidence in support of the existence of a unique population of cells in the deep subepicardial layers of the canine ventricle (M cells). Action potentials recorded from M cells display a higher V_{max} and a much steeper action potential duration (APD)-rate relationship than those of endocardium or epicardium. Phase 4 depolarization, however, is never observed in M cells. In the presence study, we used standard microelectrode techniques to examine the responsiveness of M cells to agents known to induce early and delayed afterdepolarizations (EAD & DAD) and triggered activity. Quinidine (3.3 uM), 4-aminopyridine (1-5 mM), cesium (5-10 mM), amiloride (1-10 uM) and clofilium (0.1-1.0 uM) induced EADs in M cells but not in endocardium or epicardium (basic cycle length, BCL=1.5-5 sec; $[K^+]_o$ = 2.5-4 mM). Norepinephrine (0.1-10 uM), and acetylstrophanthidin (5 x 10^{-8}-10^{-7} g/ml) induced prominent DADs and triggered activity in M cells (BCL = 250-500 msec) but not epicardium or endocardium. CONCLUSION: Deep subepicardial cells (M cells) display electrophysiologic features intermediate between those of Purkinje fibers and other myocardial cells.

8.2

PINACIDIL-INDUCED REENTRANT ARRHYTHMIAS IN ISOLATED CANINE VENTRICULAR EPICARDIUM

Jose M. Di Diego and Charles Antzelevitch. Masonic Medical Research Laboratory, Utica, NY 13501.

Pinacidil is known to augment a time-independent outward current by activating ATP-regulated K+ channels. Activation of these channels is thought to be responsible for increased K+ permeability under conditions of ischemia or hypoxia, and may play a role in arrhythmogenesis. We have previously shown that canine ventricular epicardium (EPI) is more sensitive to ischemia than endocardium (ENDO) in part because of the presence of prominent transient outward current (Ito) in EPI but not in ENDO. In the present study we used standard microelectrode techniques to study the effects of pinacidil (1.5-3 uM) on these two tissue types. In ENDO, action potential duration (APD;90%) and refractoriness abbreviated by 8.0+-2.3%. Pinacidil induced nonhomogeneous changes in EPI. At some sites, pinacidil induced an all or non repolarization and the end of phase 1 resulting in 55.5+-8.7% abbreviation of APD and refractoriness. Adjacent to these were sites at which the dome was maintained with only minor changes in APD and refractoriness. Under these conditions, premature stimulation induced reentrant excitation in EPI. CONCLUSION: Low levels of pinacidil, like ischemia, produce a marked dispersion of repolarization and refractoriness in EPI as well as between EPI and ENDO leading to the development of reentrant arrhythmias.

MECHANISMS OF MUSCLE CONTRACTION TUESDAY

11.1

MUSCLE CONTRACTION MECHANISM THEORY: A SIMPLE ENGINEERING ANALYSIS OF MYOPLASMIC SURFACE TENSION.

Alexander F. Metherell. MRI Centers, 1930 Old Tustin Ave., Santa Ana, California 92701

A disarmingly simple engineering hypothesis is developed which may explain the independent force generator that is at work in muscle. There are two universally accepted engineering assumptions that the load is (1) carried in the filaments and (2) is transferred through stress in the cross-bridges which lead inevitably to the conclusion that the independent force generator must be located in the cross-bridges. For engineering reasons we now believe these assumptions to be false. *External work is done by muscle only by going from a higher to a lower mechanical energy state.* Therefore, *movement towards greater filament overlap is movement towards a lower mechanical energy level.* All fluid surfaces contain surface energy in the form of surface tension. The myoplasmic fluid interface at the fluid-filament boundaries is considered and there are 4 reasons to expect that *the surface tension (energy) in the region of overlap will be lower than in the region of no overlap, therefore, it necessarily follows that contraction must occur.* Calculations show that this mechanism is fully capable of generating forces equal to the maximum force that muscle is known to produce. The contractile force is carried by the fluid surface, not the filament. During contraction the filament is in a state of compression, not tension. There is no mechanical connection required between the actin and myosin thus the forces are not transferred through the cross-bridges. Pressure within the myoplasmic fluid is at all times essentially zero.

11.2

MYOSIN LIGHT CHAIN PHOSPHORYLATION COOPERATIVELY ACTIVATES CROSSBRIDGE CYCLING IN SMOOTH MUSCLE. M.J. Siegman, T. Vyas, S. Mooers, S. Narayan, T.M. Butler. Jefferson Medical College, Philadelphia, PA 19107

In smooth muscle, phosphorylation of the myosin light chain can initiate the cyclic interaction of myosin with actin resulting in force generation. Maximum force output can occur with low levels of phosphorylation, and under constant force conditions, the velocity of crossbridge cycling can vary. We determined the quantitative relationship between phosphorylation of the myosin light chain and the fraction of myosin molecules that increase their rate of ATPase activity during contraction of permeabilized rabbit portal vein. Single turnover experiments were performed to directly measure the rate of nucleotide diphosphate release from myosin. Either at rest or during the plateau phase of an isometric contraction under specific conditions of phosphorylation, the muscle was incubated in either formycin triphosphate (FTP) or ^{14}C-ATP, followed by a chase in a solution containing excess ^{3}H-ATP. Nucleotide diphosphate release, as measured by the fraction of total myosin that has FDP or ^{3}H-ADP bound, was biphasic and complete in about 30 min in the resting muscle. However, when more than 80% of the myosin light chain was phosphorylated, the nucleotide diphosphate release rate was faster and complete in 2 min. Thiophosphorylation of less than 20% of the total myosin light chain caused maximum release of nucleotide diphosphate. Therefore, a small degree of myosin light chain phosphorylation cooperatively activates the ATPase activity of other unphosphorylated myosin heads. Higher levels of phosphorylation which exceed that required for maximum effect on the rate of nucleotide diphosphate release, caused further increases in the ATPase rate. We conclude that a small degree of myosin light chain phosphorylation cooperatively turns on all the myosin, and further phosphorylation increases the ATPase rate. In this way the single process of myosin light chain phosphorylation may allow independent gradation of both force output and maximum shortening velocity. (Supp. HL15835 and DK37598.)

11.3

SUB-PICONEWTON-LEVEL FORCE FLUCTUATION OF ACTOMYOSIN *in vitro*. Toshio. YANAGIDA, Department of Biophysical Engineering, Osaka University, Toyonaka,Osaka, Japan.

We have developed a new system for measuring the force produced by a small number (1-100) of myosin molecules interacting with a single actin filament *in vitro*. The technique can resolve forces less than a piconewton on the sub-millisecond time scale and thus detect fluctuations of force due to the individual molecular events.

Analysis of force fluctuations (noise) is a very powerful approach toward determining kinetic characteristics of individual myosin heads interacting with actin, especially when the number of interactions is small as in the present conditions. Under isometric conditions, we have observed large force fluctuations similar to membrane current fluctuations due to channel gating in electrophysiological systems with small numbers of channels.

The force fluctuations in the isometric condition are consistent with models incorporating stochastic and independent molecular events. The Huxley (1957) model simulate the amplitude and frequency spectrum of the observed cross-bridge noise.

On the other hand, when the actin filaments actively slide fluctuations of force are much smaller. The data analysis suggestes that during sliding, for each ATPase cycle there are many force-generating mechanical interactions between actin and myosin.

11.4

SPONTANEOUS ACTIVATION OF SMOOTH MUSCLE LATE IN ISOTONIC RELAXATION. Stephens NL, A Halayko, K Rao, X Liu, H Jiang. Dept Physiol; Fac of Med, Univ of Manitoba, 770 Bannatyne Ave, Winnipeg, MB; R3E 0W3, CANADA.

While muscle contraction has been thoroughly investigated, relatively little attention has been paid to relaxation, and, such as has, has been mainly devoted to isometric relaxation. Its importance, especially in disease states, however, could be quite considerable. In hypertensive blood vessels prolonged relaxation has been reported and said to contribute to the developed hypertension. We have conducted studies of isotonic relaxation as these are more relevant to broncho- or vasodilatation than those of isometric. We developed an index of isotonic relaxation of canine tracheal smooth muscle that was independent of load and of the initial length of the muscle's contractile element. We feel that this index can be used for comparing relaxation in different states of the muscle, e.g health vs disease, or in different animal species. The time course of relaxation in the figure indicates three phases: an initial curvilinear phase (convex downwards) that was related to waning of activation, a second, linear, that seemed to stem from elastic recoil of the muscle's internal resistor and a final curvilinear (convex downwards) that was due to reactivation of the muscle. This last seems to be the first report of such a phenomenon. Zero load clamping studies confirmed that the maximum velocity of unloaded shortening (Vo) which had shown a progressive fall (V_2,V_3 in the figure) increased again (V_4,V_5); the latter would slow the relaxation rate. Biochemical studies revealed an increase in myosin light chain phosphorylation at the same time as the increase in V_o during relaxation. (Supported by an operating grant from the Canadian Respiratory Health Centre of Excellence; JH was the recipient of a fellowship from the Medical Research Council of Canada).

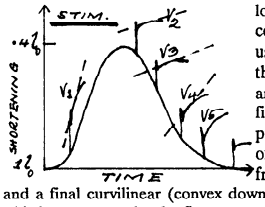

11.5

STOCHASTIC SIMULATIONS OF *IN VITRO* MOTILITY. Joseph B. Patlak and David M. Warshaw. Department of Physiology and Biophysics, University of Vermont, Burlington, VT 05405.

The *in vitro* motility assay measures actin movement on a myosin-coated coverslip, where movement depends upon relatively few myosin molecules. We have generated a stochastic simulation of myosin's (<500 heads) interaction with an actin filament. The simulation is based on the kinetic scheme for the actomyosin ATPase cycle in solution at 20° C. and low ionic strength, with the following additional assumptions: 1) Myosin crossbridges are independent, except during motion; 2) Most rate constants were derived from the ATPase cycle's rates in solution; 3) All rate constants are independent of strain or position; 4) Motion is generated as a discrete quantal step, due to a rapid conformational change in force generating bridges; 5) Non-force generating states impose a resistive load proportional to their binding strength. The simulation follows each myosin molecule as it switches between discrete conformations, each of which is occupied for a randomly distributed period of time set by the rate constants for leaving that state. For motion to occur, the total force generated by a population of bridges at any time must exceed the total resistance (or external force) applied to the filament. The simulated step rate (i.e. velocity) increases with crossbridge number, but saturates at a maximum value above 20 bridges due to the internal resistance of strongly and weakly bound states of myosin. The maximum rate of movement for >20 bridges was about 360 steps/second. At this rate, each crossbridge spends about 5% of its cycle time in force production and consumes ATP at approximately 20 s^{-1}. The simulation predicts standard force-velocity relations, reproduces the [ATP] dependence of both ATPase activity and actin filament velocity, and accurately describes the observed maximum velocity with mixtures of different types of myosins. The behavior of the simulation, as constituted, is consistent with observed actin filament velocity if steps are 10-20 nm in length.

11.6

THERMODYNAMIC STUDIES ON CARDIAC ISOMYOSINS. George Kaldor and David R.Hoak. VAMC Allen Park 48101 and Dept.Path. Wayne State Univ. Med. School,Detroit,MI,48102.

The thermodynamic efficiency of the cardiac isomyosins was studied with kinetic methods. The cardiac muscle of normal adult rabbits was the source of V1 and the heart of thyrotoxic animals was used to prepare V1. The energy of activation of the ATP-V1 complex was 14 Kcal/Mol as compared to the 9.8 Kcal /Mol obtained with the ATP-V3 complex. The decrease of entropy during the activation process was 21 e.u. with the V1 and 38 e.u. with the V3 isomyosin. The decrease of entropy of the activated complexes may indicate the tightness of fit between the enzymatic site and the substrate and/or products. In case of the ATP and/or ADP - myosin interaction this parameter may be crucial for the effectiveness of mechanochemical energy transduction. The higher energy of activation and the lower entropy loss of the V1 isomyosin - ATP interaction indicates a less efficient energy transduction than in case of the V3 - ATP interaction in each cycle of the muscular contraction. The crossbridge cycling of the V1 is higher than that of the V3 isoenzyme thus the correlation between the nucleotide -enzyme fit, crossbridge cycling and mechanochemical coupling is an interesting aspect of the contractile events.

11.7

ABSTRACT WITHDRAWN

11.8

FLUORESCENCE STUDIES WITHIN THE REGULATORY LIGHT CHAIN (LC2) OF SKELETAL MYOSIN. B.D. Hambly, W. Boey, E. Moisidis and C.G. dos Remedios. Anatomy Dept., Sydney University, 2006 Australia.

The LC2 of skeletal myosin lies within 3.5 nm of the head-rod junction (Katoh & Lowey,1989 J. Cell Biol. 109:1549), binds one mole of cation per mole LC2, can be phosphorylated and appears to modulate the Ca^{2+} sensitivity of cross-bridge cycling in skel-etal muscle. LC2 contains two Cys (125 & 154) which can be selectively labeled with probes (Hambly *et al.*, 1991 Biophys. J. 59:127) We have bound a donor-acceptor pair to these two Cys to use fluorescence resonance energy transfer (FRET) spectroscopy to measure the distance between these Cys in solution. We find the distance to be very close, in agreement with crosslinking studies (Huber *et al.*, 1989 Bio-chem. 28:9116). We also find that the fluorescence intensity of these probes does not change with Ca^{2+} binding, consistent with structure predictions that the cation site is located in the other (N-terminal) domain of the putative dumbell shaped LC2 (Bechet & Houadjeto, 1989 BBA 996:199). 50% of myosin LC2 has been successfully exchanged with labeled LC2, allow-ing the spatial relationships between residues within LC2 and other myosin probe sites to be investigated. Supported by NH&MRC of Australia.

11.9

TIME RESOLVED X-RAY DIFFRACTION MEASUREMENTS IN SINGLE INTACT MUSCLE FIBRES. Y.Maéda, C.C.Ashley, M.A.Bagni, G.Cecchi & P.J.Griffiths. EMBL at DESY, D-W2000 Hamburg 52, Germany.

Single intact muscle fibres from *Rana temporaria* were tetanised during simultaneous measurement of sarcomere length by laser diffraction and equatorial X-ray diffraction intensities. Synchrotron radiation (beam dimensions 0.3x4mm, wavelength 0.15nm) provided sufficiently strong equatorial reflexions for 5 ms time resolution of intensity changes and lattice spacing. Under length-clamped isometric conditions, both *10* and *11* equatorial signals lead tension during the tetanus rise by 15 ms (Ashley *et al.*, 1989, *J.Physiol.* **418**:58P). This can be explained by a low force attached crossbridges state preceding the force step in the crossbridge cycle. During isometric relaxation, force declines faster than equatorial signals, which indicates a low force state is also entered prior to relaxation. Fibre stiffness (4kHz), a putative indicator of crossbridge attachment, shows similar behaviour to the equatorial signals under isometric conditions. The rise of force is accompanied by a compression of the filament lattice whose time course is slower than that of tension.

During unloaded shortening, equatorial signals changed only to 60% of their plateau values. Steady state intensities during shortening were attained later than steady state force. Stiffness measurements did not agree with change in equatorial signals, stiffness falling to 30% of the plateau value (Griffiths *et al.*, 1991, *Biophys.J.*, **59**:567a). This suggests crossbridge propinquity to the actin filament during shortening does not necessarily signify a strong mechanical bond. During isometric tension recovery from shortening, equatorial signals again led tension. At the onset of unloaded shortening, the lattice expanded rapidly, but the subsequent compression during isometric tension recovery again slower than the recovery of tension (Cecchi *et al.*, 1990, *Science*, **250**:1409). Such behaviour is consistent with a radial, compressive component of crossbridge force. Small quick stretches and releases (<0.5%) completed in <1ms produced no equatorial signals within the time resolution of our present measurements.

11.10

CHEMICALLY SKINNED GUINEA PIG TAENIA COLI: THE BINDING AND POSSIBLE ROLE OF CREATINE KINASE. J.F. Clark, P. Mateo, Z. Khuchua, and R. Ventura-Clapier. Physiology Cellulaire Cardiaque, INSERM U-241, Université Paris-Sud (Bat. 443), Orsay France.

Activity and role of creatine kinase (CK) associated with contractile proteins of smooth muscle have been investigated using skinned guinea pig taenia coli fibers. Total CK activity was 163 ± 22 IU/ g ww from the BB, MB, and MM isoforms (BB-CK being the predominant isoenzyme). In Triton X-100 skinned fibers, BB-CK was specifically associated with the myofibrils, representing 22 percent of the preskinned CK activity. When relaxed fibers were exposed to pCa 9 in the presence of 250 µM ADP, 0 ATP, and 12 mM PCr, tension was unchanged, but changing to pCa 4.5 caused the fibers to generate 59.0 ± 5.2 percent of maximal tension. When a high-tension rigor state was achieved after activation (250 µM ADP, 0 ATP, 0 PCr, and pCa 9), the addition of 12 mM PCr effected significant relaxation. These observations implicate an endogenous form of BB-CK associated with the myofilaments which is capable of producing ATP for submaximal tension generation and significant relaxation from rigor conditions. It was also shown that ADP is bound to the myofibrils and available for rephosphorylation by BB-CK. These results suggest co-localization of ATPase, MLCK, and CK on the contractile proteins of the taenia coli.

11.11

SPONTANEOUS OSCILLATORY CONTRACTION OF SARCOMERES IN MYOFIBRILS. SYNERGISTIC EFFECTS OF ADP AND INORGANIC PHOSPHATE. Shin'ichi Ishiwata, Takashi Anazawa, Takashi Fujita, Norio Fukuda and Kenji Yasuda. (SPON: Y.E. Goldman) Dept. Physics, Sch. Sci. & Engn., Waseda Univ., Shinjuku, Tokyo 169, Japan

Glycerinated striated (skeletal and cardiac) muscle fibers spontaneously oscillate under partial activation with, for example, submicromolar concentrations of free Ca^{2+}. We have recently found new conditions for tension oscillation under which every sarcomere spontaneously oscillates; the coexistence of ATP and its hydrolytic products, ADP and inorganic phosphate (Pi) was required for this oscillation (named SPOC), but Ca^{2+} was not. The "state"-diagram obtained against the concentrations of MgADP and Pi in the presence of MgATP suggested that SPOC is a third state of muscle located in between the contracting and relaxing states. Here, we have studied the synergistic effects of ADP and Pi on the dynamic properties of SPOC by using glycerinated psoas myofibrils of rabbit and glycerinated cardiac muscle of bovine heart. For this purpose, we have devised a simple method to manipulate single myofibrils with a pair of glass microneedles, to observe the space-time pattern of SPOC and to measure the tension oscillation, under an inverted phase-contrast microscope with an image analysis. We will report the relationship between the oscillations each sarcomere length and tension under SPOC conditions, the effects of load on the period of SPOC and the similarities between SPOC and the oscillation with Ca^{2+} and so on.

11.12

KINETIC STUDIES OF THE STATE CHANGE OF THE MUSCLE THIN FILAMENT. Y. Ishii and S.S. Lehrer SPON: F.Sreter Boston Biomedical Research Institute, Boston, MA 02114

Biochemical studies have shown that binding of myosin subfragment 1 (S1) to reconstituted thin filaments shifts the equilibrium between a "turned-off" and a "turned-on" thin filament state. The state change has been directly monitored with fluorescence probes on Cys-190 of tropomyosin. In this study, the kinetics of the state change monitored by the excimer fluorescence of pyrene-labeled tropomyosin was determined during ATP-induced S1 dissociation from the actin-tropomyosin filament measured by the decrease in the light scattering (l.s.). At low concentration of ATP (5uM), the l.s. decreased with $t_{1/2}$~30ms, but the fluorescence decreased only after a lag of ~30ms, in agreement with the non-linear relationship between the state change and the S1 binding. When the l.s. change was complete (at 0.1s), only half of the fluorescence change was complete, indicating that the rate of the state change is slow as compared with dissociation of S1. At high concentration of ATP (0.1mM) where S1 dissociated within the mixing time (a few ms), most of the fluorescence had not yet changed and decreased with $t_{1/2}$~10ms. Therefore, the state change from the "turned-on" state to the "turned-off" state is delayed after dissociation of S1, which may be important in the regulation of muscle contraction and relaxation.

11.13

THE EFFECT OF ACTIN-MYOSIN LATTICE SPACING ON FORCE GENERATION IN SKELETAL MUSCLE. Yan Zhao and Masataka Kawai. Depart of Anatomy, University of Iowa, Iowa City, IA. 52242

The actin-myosin lattice spacing of chemically skinned rabbit psoas fibers was osmotically compressed by dextran T-500, and the effects of MgATP and phosphate (Pi) ions were studied on exponential processes (B) and (C) with the sinusoidal analysis technique at fixed dextran concentrations. Our earlier results indicate that the process (C) characterizes the cross-bridge detachment step, and the processes (B) characterizes the power stroke step AMDP ⟶ AM*DP (A=actin, M=myosin, D=MgADP) which precedes Pi release. At a low level compression (0-15%) by 0-6.3% dextran, the rate constant of the reverse power stroke step decreased, and isometric tension increased to 123%. At a high level compression (19-24%) by 9-11.7% dextran, the rate constant of the power stroke step decreased, and isometric tension changed to 121-102%. Evidently, the myosin heads have an increased difficulty in performing the power stroke at the high level compression. In both cases, the decreases in the rate constants were consistent with the changes in isometric tension. The association constant of Pi to the cross-bridges in the AMD* state, and that of MgATP to the AM state were little affected by the compression. The compression had smaller effects on the detachment step of cross-bridges. Our results demonstrate the significance of the actin-myosin lattice spacing in promoting the power stroke reaction and its reverse reaction.

11.14

A SIMPLE STOCHASTIC MODEL FOR MOTOR PROTEINS. S. Leibler[1] and D.A. Huse[2]. [1]Centre d'Etudes de Saclay, 91191 Gif-sur-Yvette, France [2]Bell Laboratories, Murray Hill, NJ 07974, USA. SPON: W.W. Webb

We construct a "minimal" 4-state stochastic model which explains in a unified way many of the results obtained by *in vitro* studies of both myosins/actin and kinesins or dyneins/microtubule systems. Analytical solutions of steady-state equations for a large number N of motor proteins interacting with a fiber: (i) give observed hyperbolic laws for the sliding velocity, v, and the ATPase activity, V, as function of the ATP concentration, [ATP]; (ii) explain why the ratio, ω, of the concentrations for half-maximal v and half-maximal V is large (~ 10 – 20) for muscle myosins (Harada et al (1987) *Nature* **326**, 805) and predict it to be small (~ 1 – 2) for kinesins; (iii) provide a possible explanation for a large apparent step size observed for myosins by Yanagida et al. ((1985), *Nature* **316**, 366) in contrast with other measurements (Toyoshima et al. (1990) *P.N.A.S.* **87** 7130). Analysis of the model for small N allows us: (a) to calculate the number of motors N^* for which v saturates; (b) to show that for large [ATP]: $N^* \simeq \omega$, i.e. it is again large for myosins and small for kinesins. This last result is closely connected with another implication of our 4-state model, namely that — in contrast to muscle myosins or flagellar dyneins — kinesins spend a large proportion of time in the strongly attached state (in agreement with assays results (Block et al. (1990) *Nature* **348**, 348)). A simple generalization of the model, for which the rates are linearly dependent on the strain, leads to the Hill's law and related laws for muscle efficiency (Hill (1938) *Proc. Roy. Soc.* **B126**, 136).

11.15

INCREASED CROSS-BRIDGES AND FORCE INCREASE THE CALCIUM AFFINITY OF TROPONIN IN BARNACLE MUSCLE FIBERS. A. M. Gordon and E. B. Ridgway. Departments of Physiology and Biophysics, University of Washington, Seattle WA 98195 and Medical College of Virginia, Richmond VA 23298.

If an aequorin injected single muscle fiber from the barnacle Balanus nubilus is shortened decreasing the force during the declining phase of the Ca transient, "extra" free Ca is observed. We (Ridgway and Gordon, 1984) hypothesized that this "extra" Ca is from Ca-troponin (CaTn); the Ca affinity being decreased by cross-bridge detachment accompanying muscle shortening. Assuming that the peak amplitude of the "extra" Ca on shortening is proportional to CaTn at the time of shortening, the time course of the peak "extra" Ca is a measure of the time course of CaTn. Measuring CaTn in this manner and the free Ca from the aequorin signal, we find that a single apparent CaTn affinity (K_{app}) can not fit these data during the entire twitch, but only while force is near its peak and relatively constant. As the peak force is increased (by increasing the stimulus), the calculated K_{app} increases steeply. With the change only in CaTn dissociation,

$$k_{off}=k_{off,0}[0.1 + 0.9\exp(-Force\{kg/cm^2\}/0.3)].$$

Using this function, calculations of the free and bound Ca, the force and the "extra" Ca seen with a step decrease in force during the twitch show good agreement between the measured/calculated time courses/magnitudes. Thus the "extra" Ca on shortening is consistent with increased Ca affinity of Tn with increased force/cross-bridge attachment, particularly at low force levels and can account for some cooperative Ca activation of contraction (calculated Hill coefficient, 1.84). (Supported by NIH NS08384, AM35597 and Virginia Heart Assoc.)

11.16

COMPARISON OF THE MECHANICAL AND ELECTROPHYSIOLOGICAL EFFECTS OF TWO ISOQUINOLINE ALKALOIDS ON RAT CARDIAC TISSUE. M.J. Su*, P.J. Liu, Y.C. Nieh and J.H. Lee+. Department of Pharmacology, College of Medicine, National Taiwan University and National Institute of Chinese Medicine+, Taipei, Taiwan.

Our previous work found that some isoquinoline alkaloids from Chinese herbs exerted electrophysiological actions like quinidine. This work was to examine the actions of 3,4-dihydroxybenzyl 6,7-dihydroxy-1,2,3,4-tetrahydroisoquinoline (CSH109) and 2-bromo-3,4-dimethoxy-benzyl 6,7-dimethoxy-1,2,3,4-tetrahydro-isoquinoline (CSH118). In rat right atria, left atria and right ventricular strips, CSH109, at concentrations from 0.3 to 3 uM, increased contractions dose-dependently. Voltage clamp study proved that CSH109 (1.5 uM) increased calcium inward current (I_{Ca}) of rat ventricular cells significantly. These effects of CSH109 were antagonized by propranolol. In contrast to CSH109, CSH118 (0.3 to 3 uM) failed to increase contractions of the preparations. At higher concentration (9 to 45 uM), CSH118 reduced contractions and membrane excitability. Voltage clamp study in ventricular cells found that CSH118 (9 uM) exerted stronger inhibition of sodium inward current (I_{Na}) and calcium inward current than quinidine. These results indicate that CSH109 exerts positive inotropic and chronotropic effects by activation of beta-adrenergic receptor. CSH118, however, reduces muscle excitability and contractility by inhibition of I_{Na} and I_{Ca}.

11.17

VANADATE AND PHOSPHATE PROBE THE ENERGETICS OF CROSS-BRIDGE STATES DURING THE FORCE PRODUCING STROKE IN SKELETAL MUSCLE. Greg Wilson, Sarah Shull, Ed Pate & Roger Cooke, Biochemistry & Biophysics, UCSF, San Francisco, Ca., 94143

Vanadate (V_i), a phosphate (P_i) analog, inhibits force in skinned rabbit fast-twitch muscle fibers. The figure shows force versus $\log_{10}[V_i]$ in 5 and 50mM P_i. In 50mM P_i force was 74% compared with 5mM P_i. Force declined linearly in $\log_{10}[V_i]$ from 100% to 0% at both $[P_i]$ with a $10^{2.8}$-fold increase in $[V_i]$ (25°C, pH 7, 210mM ionic strength). The curves show that P_i competes with V_i for binding to the myosin head, and fibers were less sensitive to V_i in 50mM P_i. The linearity of the decline of force with $\log_{10}[P_i(V_i)]$ can be explained with a model in which the free energies of cross-bridge states depend on [ligands] (Pate & Cooke, Pflugers Arch. 414, 73 (89)). This model predicts that P_i and V_i inhibit force by lowering the number of strongly bound A.M.ADP states. Since it takes 2.8 $\log_{10}$ units of V_i to abolish force at either $[P_i]$, this corresponds to about 16kJ mol^{-1}, which is less than the free energy drop expected for muscle to work efficiently.

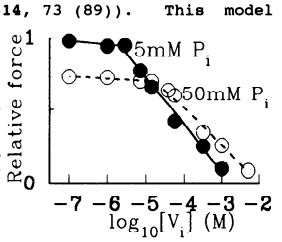

MDA (GW) & USPHS AM30868.

11.18

STIFFNESS CHANGES ASSOCIATED WITH EXERCISE-INDUCED MUSCLE INJURY IN HUMANS. J.N. Howell, R. Conatser, G. Chleboun and J. Cummings. Ohio Univ. Coll. Osteopathic Med., Athens OH 45701

To examine changes in muscle stiffness which result from exercise known to produce injury we used a device, which holds the arm in the horizontal plane and moves it stepwise through the entire range of elbow motion. Subjects were instructed to relax, and surface EMG was monitored in both elbow flexors and extensors. Torque required to hold the elbow at each successive angle was converted to muscle tension with the model of van Zuylen et al. (J. Biomech. 21:183, 1988). Muscle injury was induced when subjects repeatedly lowered (typically <10 reps. in each of 3 sets) with their elbow flexors a load, normalized to 90% of their own strength, until they could no longer control the rate of lowering. Length-tension plots were linear between approx. 90° and 140°. Following exercise the stiffness in this range more than doubled and remained high for 3 days. No onset delay occurs as it does for swelling or soreness. Return to control values is faster for stiffness than for strength. The stiffness changes may reflect low level contractile activity in damaged fibers, undetectable by EMG. (Supported by Am. Osteopath. Assn.)

11.19

MUSCLE FATIGUE IN THE FROG SEMITENDINOSUS: THE ROLE OF INTRACELLULAR pH. LaDora V. Thompson, Ed M. Balog and Robert H. Fitts. Marquette University, Milwaukee, WI 53233

The purpose of this study was to utilize glass microelectrodes to characterize the intracellular pH (pH_I) before and during recovery from fatigue in the frog semitendinosus muscle. A second objective was to evaluate the relationship between pH_i and contractile function. The frog semitendinosus (ST) muscle was fatigued by direct electrical stimulation with 100ms, 150 Hz trains at 1/s for 5 min. Peak tetanic tension (P_o) was reduced to 8.5% of initial tension and recovered in a biphasic manner by 40 min. Resting pH_i was 7.00 ± 0.02 (n=37), and declined with fatigue to 6.42. During recovery pH_i returned to the pre-fatigue value by 25 min. The pH_i recovery was highly correlated to the slow phase of P_o recovery ($r=0.97$, $p\leq0.001$). The mean resting membrane potential (V_m) was -78 ± 1.0 mV (n=42), and following fatigue was depolarized to -67 ± 4 mV. Both the peak rate of twitch tension development (+dp/dt) and decline (-dp/dt) were highly correlated to pH_i during the slow phase of recovery. Contraction time (CT) and one-half relaxation time (1/2 RT) increased significantly and recovered in two phases. The second slower phase of recovery for CT and 1/2 RT were significantly correlated to pH_i. In conclusion, the high correlations between force, ±dp/dt, CT, 1/2 RT and pH_i during recovery from fatigue support the hypothesis that the slow phase of recovery is at least partially linked to an elevated H^+ ion.

11.20

MAXIMAL SHORTENING VELOCITY AND ATPase ACTIVITY OF SINGLE SLOW- AND FAST-TWITCH RAT MUSCLE FIBERS. Jane M. Schluter, Kerry M. McDonald and Robert H. Fitts. Marquette University, Milwaukee, WI 53233

One objective was to test the hypothesis that the fast type IIb fiber exibits a higher Vmax and ATPase activity than the fast type IIa fiber. Vmax was determined by the slack test and fiber ATPase measured fluorometrically. The Vmax (7.9 ± .18 fl/s) of the type IIb fiber was significantly greater than the type IIa fiber (4.4 ± .21 fl/s) and a similar difference existed in the ATPase activity (927 ± 70 vs 760 ± 60 $uM.min^{-1}.mm^{-3}$). A second objective was to determine the effect of regular endurance exercise on fiber Vmax and ATPase activity. The training program consisted of treadmill running 2 hr/day, 5 day/wk up a 15% grade at a speed of 27m/min for 6-12 wk. The Vmax of the trained soleus type I fibers was significanlty greater (33%) than the control fibers. Concomitantly, there was a significant increase (33%) in the fiber ATPase activity following training. The exercise induced increase in the Vmax was highly correlated with ($r = 0.76$) and likely caused by the elevated fiber ATPase. The fast type IIa and IIb fibers were not significantly altered by the exercise program. In conclusion, this study clearly demonstrates a functional difference between the fast type IIa and IIb fibers, and establishes that endurance exercise-training increases the fiber ATPase and Vmax of the slow type I fiber. Supported by NIH AR39894.

11.21

ATP HYDROLYSIS AND MYOFIBRIL SHORTENING Edwin W. Taylor
Univ. of Chicago, Chicago, IL 60637

The transient phase of ATP Hydrolysis at 20° by rabbit back muscle myofibrils in presence of calcium consists of a small phosphate burst phase (0.2 to 0.25 moles per head) and rate 80 to 100/sec, followed by a steady state rate V of 12 to 15/sec per myosin head over the first 100 msec. Based on a four state model and an association of 0.5 for cross bridges, the effective rate constant for product release is greater than 100/sec. The velocity of shortening was determined by using the quench flow apparatus to stop shortening by mixing with 2% glutaraldehyde, 0.4 M acetate buffer. The velocity at sarcomere lengths of 2.2 to 2.0 um was 1.5 to 2 um/sec per half sarcomere. The simplest model of shortening predicts that the velocity u is given by u = kd where k is the rate constant from transient kinetics and d is the step distance. The result is 10 to 20 nm. Steady state measurements are interpreted by the equation u/V = d/f where f is a factor to be determined from experiments and/or models. If f = V/k (the duty cycle ratio) then u = kd. The discrepancy in determinations of d arises from very different estimates of f.

11.22

POTASSIUM (K) CHANNEL INHIBITORS CAUSE ENDOTHELIUM INDEPENDENT PULMONARY ARTERIAL VASOCONSTRICTION.
Stephen L. Archer, Joseph M. Post, Joseph R. Hume, Daniel P. Nelson, E. Ken Weir, Minneapolis VAMC, Mn 55417 and Dept. Physiology, Reno, NV.

Hypoxia alters regional blood flow through the lung by an unknown mechanism. Recent studies of the type 1 cell of the carotid body, suggest that changes in O_2 tension may modulate K channel activity. To evaluate the hypothesis that K channels in pulmonary artery (PA) smooth muscle might also function as O_2 sensors, the effects of 2 K channel inhibitors, 4 aminopyridine, (4AP) and tetraethylammonium (TEA) on PA tension and pressure were assessed in canine PA rings and rat lungs. TEA and 4AP caused concentration-dependent increases in ring tension. TEA increased PA pressure in a dose-dependent manner. Vasodilatation caused by the K channel agonist pinacidil was completely prevented by TEA and 4AP. Endothelium-denuded rings constricted to hypoxia and TEA. In freshly dispersed canine PA smooth muscle cells, using the whole cell variation of the patch clamp technique, 4-AP (10mM) inhibited K currents. Single channel studies are necessary to determine whether hypoxia and the K channel inhibitors are acting on the same K channels. These data support the hypothesis that inhibition of a K channel could lead to pulmonary vasoconstriction.

11.23

KINETICS OF CROSS-BRIDGE CYCLING IN THE PRESENCE OF MGADP IN ALPHA-TOXIN PERMEABILIZED SMOOTH MUSCLE CELLS. Eiichiro Nishiye, Avril V. Somlyo, Katalin Török* and Andrew P. Somlyo,
Department of Physiology, University of Virginia, Charlottesville, VA22908, *National Institute for Medical Research, London,U.K.

The rate of detachment of cross-bridges in α-toxin permeabilized guinea-pig portal vein was investigated using laser flash photolysis of P3-1(2nitrophenyl)ethyladenosine-5'-triphosphate(caged ATP) to clarify the rate of cross-bridge cycling under near physiological conditions. Isometric tension and in-phase stiffness from rigor state were monitored in muscles upon photolysis of caged ATP in the absence of Ca^{2+}. The estimated concentration of ATP released from caged ATP by HPLC was 1.8 mM. The rate of relaxation during the initial 0.2 seconds after photolysis was approximated by 2 exponential functions with rate constants of 31.8, 0.99 s^{-1} and relative amplitudes of 0.22, 0.78; multiple exponential functions were needed to fit longer intervals. The rate of relaxation was not affected by changing the incubation time in rigor solution from 20- 40 minutes, but increased by 18mU/μl Apyrase(ATP and ADPase). MgADP dose dependently decreased the amplitude of the initial phase of relaxation and induced a plateau phase after the initial rapid phase. Inorganic phosphate (Pi) did not affect the rate of the initial rapid phase, but accelerated the slow phase. Stiffness decreased during the plateau phase, suggesting that tension per cross-bridge increased. Analyses of the effects of MgADP and Pi on the kinetics of the cross-bridge cycle are in progress. This work was supported by the fellowship from HFSPO to E.N. and by HL15835 to the Pensylvania Muscle Institute.

11.24

RATE OF REGENERATION OF 12 nm POWER-STROKE AFTER SUDDEN SHORTENING OF TETANIZED FIBRE FROM FROG MUSCLE. G. Piazzesi, M. Linari and V. Lombardi. Dpt. Scienze Fisiologiche, Università di Firenze, Firenze, Italy. SPON: Y.E. Goldman.

Quick release experiments in intact fibres (Huxley & Simmons, Nature 233, 533-538, 1971) indicate that the sliding distance over which a cross-bridge remains attached to actin, while produces force and shortening is about 12 nm. We determined the rate at which a cross-bridge subjected to rapid shortening can regenerate "Huxley & Simmons" power-stroke by imposing test step releases at various times (2-20 ms) after a conditioning release on tetanized fibres dissect from tibialis anterior muscle of the frog (Rana esculenta) (4 °C, sarcomere length 2.1 μm). At 2 ms after a conditioning step of 5 nm, the test T_2 curve (the plot of tension attained at the end of quick recovery versus step size) was less convex and was shifted to the right, with respect to that obtained with single steps, by an amount roughly similar to the size of conditioning step; at successive times the curve progressively (time constant about 7 ms) regained the characteristics of the control T_2 curve. Increase in size of the conditioning step reduced the number of attached cross-bridges undergoing this process. These results indicate that after the quick phase of tension recovery following a step release, cross-bridges detach and readily reattach farther along the actin filament. The power output of shortening muscle can be explained according to the kinetics of this process.

11.25

EFFECTS OF ALUMINOFLUORIDE ON SKINNED MUSCLE FIBER STIFFNESS. P. Bryant Chase, Donald A. Martyn, Martin J. Kushmerick, and Albert M. Gordon. University of Washington, Seattle, WA 98195.

Aluminofluoride complex (AlF_x) is an analog of orthophosphate (Pi) (Chabre, 1990, TIBS 15:6) which inhibits maximum Ca-activated force of skinned fibers from rabbit psoas muscle. The inhibition of fiber force reverses (10 - 20 min; 12°C) in activating solution (Chase & Kushmerick, 1990, in: Muscle and Motility, vol. 2, G. Maréchal & U. Carraro, eds., pp. 247). Fiber stiffness was obtained by measuring force responses to step (instantaneous force change, T1) and sinusoidal (1 kHz; 0.05 - 0.1% ptp) changes in fiber length. Sarcomere length (s.l.) changes were obtained from the centroid of a He-Ne laser diffraction first order. In activating solution (pCa 4; no added Pi) with 10 mM F and 200 μM Al added, steady-state isometric force was 18 - 25% of control while stiffness was 32 - 39%; i.e., stiffness was inhibited less than force. Similar results were obtained with both step and sinusoidal length changes. These results provide evidence for the existence of low- (or non-) force generating cross-bridges which contribute to stiffness (Martyn & Gordon, 1988, Biophys. J. 53:568a) and which have Pi-analog bound since the apparent off-rate for AlF_x, derived from recovery of force, is slow (minutes) relative to the time scale of the stiffness measurements. Supported by NIH grant HL31962.

11.26

COMPUTER SIMULATIONS OF MECHANICAL TRANSIENTS IN SKELETAL MUSCLE FIBERS H. Shuman, J.A. Dantzig, Y.E. Goldman. Penna. Muscle Institute, Univ. of Penna, Phila.,PA 19104

The Pate and Cooke (P-C) theory[1] can explain the effects of [ATP], [ADP] and [phosphate] ([Pi]) on active force and shortening velocity. However, it does not correctly predict mechanical responses to rapid length steps[2]. Quick length changes shift the strain-dependent population distribution of cross-bridge states along the strain axis, and the recovery reflects the redistribution kinetics. For small steps, the largest recovery amplitudes occur at strains corresponding to inflection points in the distribution where populations of two kinetically connected states are nearly equal. The return to steady state at each inflection point is dominated by a single rate process. Mechanical transients[2,3] are described by at least 4 rate processes. The P-C model only accounts for 3 and does not describe the faster part of the quick recovery (phase ph2f in scheme). An extra term can be gained by adding either a new transition between existing states or a new state.

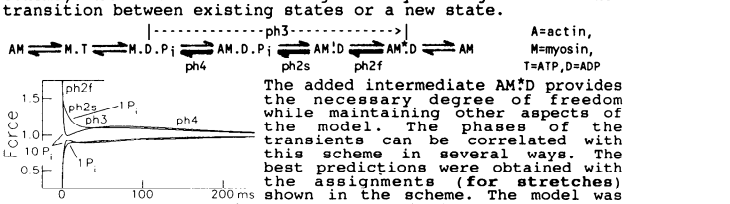

The added intermediate AM*D provides the necessary degree of freedom while maintaining other aspects of the model. The phases of the transients can be correlated with this scheme in several ways. The best predictions were obtained with the assignments (**for stretches**) shown in the scheme. The model was used to simulate transients at 1 mM and 10 mM Pi (Fig.) in reasonable agreement with the transients reported by Dantzig *et al.*[3]. Supp: NIH HL15835 to P.M.I.. [1]Pate & Cooke, *J. Musc. Res. & Cell Mot.* 10:181, 1989. [2]Huxley & Simmons, *Nature* 233:533, 1971. [3]Dantzig *et al.*, *Biophys. J.* 59:36a, 1991.

11.27

AT LOW TEMPERATURE AND IONIC STRENGTH AM-T --> AM-D-P IS THE RATE LIMITING STEP OF SKELETAL ACTOMYOSIN-S1 ATP HYDROLYSIS, Betty Belknap, Xing-Qiao Wang, Xue-Zhong Zhang and Howard D. White, Dept. of Biochemistry, Eastern Virginia Medical School, Norfolk, Va. 23507

Proposed rate limiting steps of actomyosin-S1 ATP hydrolysis are bond splitting (1), a conformation change subsequent to bond splitting (2) or phosphate release (3).

(1) (2) (3)
AM + T <==> AM-T <==> AM-D-P <==> AM-D-P'<==> AM-D <==> AM

We have measured the steady state and presteady state hydrolysis of ATP by the purified A1 isozyme of rabbit skeletal acto-myosin-S1 at conditions of very low ionic strength to maximize the rate of ATP binding and association of the steady state myosin-S1 intermediates with actin. At 4° C the steady state rate of A1-S1 ATP hydrolysis displays an unusual dependence upon [actin]. The maximum rate at 3-5 uM actin decreases to a rate that is independent of [actin] at higher concentrations. The steady state kinetics require a mechanism in which one or more steps on the actomyosin pathway are slower than the corresponding step(s) of the myosin pathway. The rate of hydrolysis of a single turnover of ATP hydrolysis [S1] > [ATP] is the same as the steady state rate at high actin concentration. Presteady state ATP hydrolysis measured under conditions where [ATP] > [S1] has a burst at low [Actin] which decreases with increasing concentrations of [Actin] to a value that is less than the limits of detection (~0.1 mole/mole). These results indicate that the rate limiting step of the ATP hydrolysis mechanism at high actin, which may emulate a contracting muscle, is the bond splitting step(1). Supported by HL41776.

11.28

ELECTRON CRYO-MICROSCOPY OF ACTOMYOSIN-S1 DURING STEADY STATE ATP HYDROLYSIS: John Trinick and Howard White, Dept. of Muscle Biology, Bristol University College of Veterinary Medicine, Langford, Bristol BS187DY, UK and Dept. of Biochemistry, Eastern Virginia Medical School, Norfolk, Va. 23501.

The primary force of muscle contraction is thought to involve some change in the myosin head while attached to actin with the energy for this coming from ATP hydrolysis. A considerable amount is know about the structure of one such attached state, the so-called strongly attached state, which occurs in the presence of ADP or in the absence of nucleotide but much less is know about the structure of the so-called weakly bound states that occur in the presence of ATP.

We have recently found conditions of low ionic-strength and moderate protein concentration where, without resorting to cross-linking, a high fraction of heads (S1) bind to actin during steady state ATP hydrolysis. The structure of this complex is being studied by electron cryo-microscopy of hydrated specimens. In the micrographs some S1 molecules are seen in the background, but we estimate from 90° light scattering experiments that approximately 70% of the S1 is bound to actin. During steady state ATP hydrolysis, the acto-myosin-S1 complex has an appearance distinct from images obtained in the absence of ATP or actin filaments alone. Preliminary analysis of the images, and of Fourier transforms calculated from them, does not reveal strong evidence of preferred conformations. Rather the data suggest a variety of structures. Micrographs of similar preparations that had been allowed to completely hydrolyze ATP have the so-called arrowhead appearance characteristic of a 45° angle of binding. Supported by research grants from AHA and MDA.

NON-MUSCLE MOTILITY

12.1

Effects of Membrane Depolarization on Neurite Outgrowth and Microtubule Polymerization Equilibria in Axons and Dendrites of Sympathetic Neurons in Culture. Charles H. Keith, Department of Zoology, University of Georgia, Athens GA.

In a number of neurons in culture, depolarization, which elevates $[Ca^{++}]_i$, is correlated with a cessation of neurite outgrowth. We have hypothesized that this effect on neurite extension occurs by means of an effect on microtubule polymerization equilibria, and have developed methods to measure polymer/tubulin ratios locally in cells. These methods are based on video densitometry of microinjected rhodamine-tubulin before and after extraction of free dimer.

We find that depolarization of rat sympathetic neurons has effects dependent on the substrate on which the cells are grown. Neurites of cells grown on laminin in the presence of serum - conditions that favor dendrite growth from these cells - retract and depress their microtubule polymerization ratio on depolarization in high K^+. By contrast, neurites grown on collagen in the absence of serum - conditions that promote the development of unipolar, axon-bearing neurons - continue growing and have unaffected polymerization ratios on depolarization. We feel that these differences between axons and dendrites are related to the differences in their microtubule-associated proteins, and may be significant in sculpting axonal and dendritic arbors during development. Supported by NS25101.

12.2

KINESIN UNFOLDS AT HIGH IONIC STRENGTH. David D. Hackney and Joelle D. Levitt. Dept. Biological Sciences, Carnegie Mellon Univ., Pittsburgh, PA 15213.

Kinesin is a molecular motor which can drive the sliding movement of membrane vesicles along microtubules (MTs). It has a MT-stimulated ATPase and shares many properties in common with the actin-activated ATPase myosin, including an overall structural resemblance. For both enzymes in the absence of activation, the rate limiting step is the release of products (ADP) and this release is accelerated by interaction with MTs or actin (Proc. Natl. Acad. Sci. U.S.A. 85, 6314 (1988)). There is high variablilty in the reported maximum ATPase rates of kinesin and this is, at least in part, due to removal of the 64 kDa β subunits (Biochem. Biophys. Res. Comm. 174, 810 (1991)). This influence of the β subunits was, however, difficult to understand in view of the proposed structural model for kinesin in which the β subunits are far removed from the head groups in an extended conformation. We now report that the 9.4 S form of kinesin is actually folded under the conditions of the ATPase assay and the β subunits are possibly in contact with the head groups and able to influence their activity. Kinesin unfolds at high ionic strength into an extended 6.5 S form. This conformation transition is stikingly similar to that undergone by smooth muscle myosin and this transition for kinesin may be involved in its regulation.

12.3

"MEASURING THE ISOMETRIC TENSION OF KINESIN MOLECULES USING THE LASER OPTICAL TRAP"
Michael P. Sheetz and Scot C. Kuo. Duke University Medical Center, Durham, NC 27710

Microtubules can be translocated by a single kinesin molecule (Howard et al., 1989 Nature 342, 154) when limiting dilutions of kinesin is adsorbed to glass in the presence of carrier proteins. By attaching latex beads as "handles" to translocating microtubules, we can reversibly stop the movement of these microtubles by a single-beam optical trap, also called laser tweezers. The optical trap uses the radiation pressure of near-infrared laser illumination to trap microscopic particles (Ashkin et al., 1987 Science 235, 1517; Nature 330, 769). The force of the optical trap was calibrated by viscous drag on latex beads and the trapping force is linear with the amount of laser illumination. Preliminary measurements indicate that the maximum force (i.e. isometric tension) of a single kinesin attachment site is about 2.0 piconewtons (10^{-7} dyne). Stalling kinesin with the laser tweezers is reversible; when trapping forces are decreased, microtubule translocation resumes. Further measurements are required for statistical analysis and would determine the cooperativity, if present, of force generation as additional kinesin molecules drive the same microtubule filament. A videotape demonstrating the technique will be shown.

13.1

AN ELECTRONIC IMAGING SYSTEM MODIFIED FOR MICROSCOPIC STUDIES OF RAPID EVENTS IN LIVE SKELETAL MUSCLE CELLS. **Stuart R. Taylor*, Ian R. Neering, Laura A. Quesenberry, and V. Arlene Morris.** Mayo Foundation, Rochester, MN 55905

Most microscopic bio-imaging systems use lenses with high NA, and sensors with high spatial resolution but relatively low temporal resolution. These are not suitable for studies of rapid events in thick, long objects like live, intact, adult muscle cells. We use relatively low NA LWD objectives to study striated muscle without obstructing its motion. Our sensors are photodiodes imbedded in small, square matrices, configured to read each pixel sequentially, and rapidly reset the sensor once the objects of interest are scanned. This allow frames of variable size to be exposed for very short times in rapid succession. Transverse spatial resolution is relatively good. But asymmetrical longitudinal spherical aberration limits 3D resolution to no fewer than many myofibrils. We made dynamic measurements of changes in cross-sectional area of skeletal muscle cells during individual contractions. The results suggest the cytoskeleton balances outwardly directed radial forces during contraction. **Supported by the Mayo Foundation, the NIH (NS 22369), the NSF (DMB-85034964), and the Australian NH & MRC.**

13.2

HIGH SPEED VIDEO MICROSCOPY: MYOCYTE STRIATION PATTERN DYNAMICS IMAGED AT A 240 Hz FIELD RATE. Kenneth P. Roos, Cardiovascular Research Lab, Dept. of Physiology, UCLA, Los Angeles, CA. 90024-1751.

The rapid motion of microscopic features and the 2-D transient modulations in intensity distributions of fluorescent probes are difficult to capture and evaluate from living cells with conventional broadcast video systems and inflexible image processing approaches. We have modified a 572H by 485V pixel format video camera for RS-170 compatible, 240 Hz operation (Roos & Parker, Proc. SPIE, 1205:134, 1990). We have coupled this high-speed camera to a widefield microscope adjusted to full numerical aperture to examine the cross-striation patterns from isolated rat cardiac myocytes. Video images of entire cells are recorded, digitized, de-interlaced and analyzed with a customized image processing system to obtain striation patterns without aliasing. Using this system, we have found that cell shortening and relaxation are smooth and synchronous in all regions of the cell during a single beat. But there are often differences in absolute striation periodicity from region to region within a cell.
Supported by HL-29671 & the Laubisch Endowment.

13.3

EVANESCENT WAVE MICROSCOPY: A SIMPLE OPTICAL CONFIGURATION FOR MOTILITY STUDIES. John M. Murray. Dept of Anatomy, Univ of Pennsylvania, Philadelphia, PA 19104-6058

The observation of filaments gliding over a lawn of adsorbed "motor" molecules, and the examination of cell-substratum contact sites are two common situations where the phenomena of interest occur very close to an essentially flat surface. Under suitable conditions, these surface phenomena can be selectively illuminated using the evanescent wave that is created at an interface where total internal reflection occurs. Material in bulk solution or in regions of the cell away from its basal surface become effectively invisible since the evanescent wave decays exponentially with distance from the interface.

A simple method of achieving evanescent wave illumination has been devised and shown to be useful for observing microtubules gliding over a surface. In contrast to previously described methods, the present arrangement has the advantage of producing circularly symmetric illumination and of utilizing only standard optical elements commonly available in cell biology laboratories.

13.4

VASOPRESSIN-INDUCED DEPOLYMERIZATION OF F-ACTIN DETERMINED BY CONFOCAL MICROSCOPY. **Richard M. Hays, Nicholas Franki, Kajsa Holmgren and Karl-Eric Magnusson. Albert Einstein College of Medicine, Bronx NY 10461 and University of Linköping Faculty of Health Sciences, Linköping, Sweden.**

Vasopressin (AVP) induces the fusion of vesicles containing water channels with the apical membrane of the toad bladder epithelial cell. There is a simultaneous a 20-30% depolymerization of F-actin. We have employed the confocal laser scanning microscope to determine where in the cell depolymerization takes place. Control bladders and bladders stimulated for 15 minutes with AVP were fixed, then stained with rhodamine-phalloidin, which selectively binds to F-actin. Vertical sections were then analyzed, and the fluorescence intensity of the apical cell segments compared to that of the lateral cell borders. In 6 paired experiments, involving more than 1,000 observations, the apex/side fluorescence ratio for control bladders was 1.84 ± 0.25 (SE), and for AVP-treated bladders 1.30 ± 0.16. The 29% decrease was significant ($p<0.01$). Thus, actin depolymerization takes place apically, in the region of vesicle fusion, and may be a requirement for fusion.